Int. J. Cancer: **122,** 124–131 (2008)

Hepatitis C virus core protein induces spontaneous and persistent activation of peroxisome proliferator-activated receptor α in transgenic mice: Implications for HCV-associated hepatocarcinogenesis

Naoki Tanaka[1,2]*, Kyoji Moriya[3], Kendo Kiyosawa[2], Kazuhiko Koike[3] and Toshifumi Aoyama[1]

[1]*Department of Metabolic Regulation, Institute on Aging and Adaptation, Shinshu University Graduate School of Medicine, Matsumoto, Japan*

[2]*Division of Gastroenterology, Department of Internal Medicine, Shinshu University School of Medicine, Matsumoto, Japan*

[3]*Department of Internal Medicine, Graduate School of Medicine, University of Tokyo, Tokyo, Japan*

Persistent infection of hepatitis C virus (HCV) can lead to a high risk for hepatocellular carcinoma (HCC). HCV core protein plays important roles in HCV-related hepatocarcinogenesis, because mice carrying the core protein exhibit multicentric HCCs without hepatic inflammation and fibrosis. However, the precise mechanism of hepatocarcinogenesis in these transgenic mice remains unclear. To evaluate whether the core protein modulates hepatocyte proliferation and apoptosis *in vivo*, we examined these parameters in 9- and 22-month-old transgenic mice. Although the numbers of apoptotic hepatocytes and hepatic caspase 3 activities were similar between transgenic and nontransgenic mice, the numbers of proliferating hepatocytes and the levels of numerous proteins such as cyclin D1, cyclin-dependent kinase 4 and c-Myc, were markedly increased in an age-dependent manner in the transgenic mice. This increase was correlated with the activation of peroxisome proliferator-activated receptor α (PPARα). In these transgenic mice, spontaneous and persistent PPARα activation occurred heterogeneously, which was different from that observed in mice treated with clofibrate, a potent peroxisome proliferator. We further demonstrated that stabilization of PPARα through a possible interaction with HCV core protein and an increase in nonesterified fatty acids, which may serve as endogenous PPARα ligands, in hepatocyte nuclei contributed to the core protein-specific PPARα activation. In conclusion, these results offer the first suggestion that HCV core protein induces spontaneous, persistent, age-dependent and heterogeneous activation of PPARα in transgenic mice, which may contribute to the age-dependent and multicentric hepatocarcinogenesis mediated by the core protein.

Key words: cell-cycle regulator; peroxisome; nuclear stabilization; heterogeneous PPARα activation

Hepatitis C virus (HCV) is one of the major causes of chronic hepatitis, and persistent infection with this virus can lead to a high incidence of hepatocellular carcinoma (HCC).[1,2] The prevalence of HCC because of chronic HCV infection has increased over the past two decades,[3,4] and chronic HCV infection has therefore been recognized as a serious disease. However, the precise mechanism of hepatocarcinogenesis during chronic HCV infection remains unclear.

Many experiments using cell culture systems have suggested the possibility that HCV core protein itself can modulate various cellular functions and can be directly linked to the development of HCV-related HCC.[5] For example, HCV core protein transforms rat embryo fibroblasts to a tumorigenic phenotype in cooperation with the H-*ras* oncogene,[6] suppresses *c-myc*-related apoptosis[7] and transcription of the *p53* gene,[8] interacts with a variety of proteins, including helicase, lymphotoxin-β receptor, or dead box protein, and modulates their functions.[9] We further established transgenic mouse lines carrying the HCV core gene, in which the core protein is constitutively expressed in the liver at levels similar to that found in chronic hepatitis C patients.[10] These mice exhibited multicentric hepatic adenomas, and developed HCCs in an age-dependent manner.[11] The livers of these mice were almost free of inflammation, necrosis and fibrosis,[10,11] suggesting that the core protein itself has a hepatocarcinogenic potential *in vivo*. However, the molecular mechanism of the development of HCC in the transgenic mice has not been fully understood.

In the livers of HCV core gene transgenic mice, an age-dependent increase in oxidative stress and resultant DNA damage were found,[12] and these effects may contribute to or facilitate the development of HCC. Another possible mechanism of hepatocarcinogenesis is continuous enhancement of hepatocyte proliferation. Cell proliferation and apoptosis are highly regulated processes for maintaining homeostasis in many organs, and during the carcinogenic process, sustained imbalance generally precedes cancer.[13,14] For example, in patients with chronic HCV infection, high hepatocyte proliferative activity relative to apoptosis may reliably predict a new development of HCC.[15] However, there is no information about whether or not hepatocyte proliferation accelerates persistently in mice carrying the HCV core gene, and no information about how the core protein promotes hepatocyte proliferation *in vivo*. In the current study, we began to examine changes in the parameters of hepatocyte proliferation and apoptosis in the transgenic mice.

Material and methods

Animals and treatments

HCV core gene transgenic mice on a C57BL/6N genetic background were produced as described earlier.[10] Because HCC developed preferentially in male transgenic mice,[11] 9- and 22-month-old male mice ($n = 8$ for either age group) were adopted. Sex- and age-matched nontransgenic mice ($n = 8$ for either age group) were used as controls. These mice were fed an ordinary diet and were treated in a specific pathogen-free state according to the institutional guidelines. For additional experiment, male wild-type mice fed a control diet containing 0.5% clofibrate for 2 weeks ($n = 8$) were used. All mice were killed by cervical dislocation and the livers were excised. When a hepatic tumor was present, it was removed and the remaining liver tissue was used. All experiments were performed in accordance with animal study protocols approved by the Shinshu University School of Medicine.

Abbreviations: AOX, acyl-CoA oxidase; CDK, cyclin-dependent kinase; DAB, 3,3'-diaminobenzidine; FITC, fluorescein isothiocyanate; HCC, hepatocellular carcinoma; HCV, hepatitis C virus; L-FABP, liver-type fatty acid-binding protein; NEFA, nonesterified fatty acid; PBS, phosphate-buffered saline; PCNA, proliferating cell nuclear antigen; PMSF, phenylmethylsulfonyl fluoride; PPAR, peroxisome proliferator-activated receptor; PT, peroxisomal thiolase; RXR, retinoid X receptor; SDS, sodium dodecyl sulfate; TUNEL, terminal deoxynucleotidyl transferase-mediated deoxyuridine triphosphate nick-end labeling.

***Correspondence to:** Department of Metabolic Regulation, Institute on Aging and Adaptation, Shinshu University Graduate School of Medicine, 3-1-1 Asahi, Matsumoto, 390-8621, Japan. Fax: +81-26-337-3094.
E-mail: naopi@hsp.md.shinshu-u.ac.jp

Received 2 May 2007; Accepted after revision 28 June 2007
DOI 10.1002/ijc.23056
Published online 31 August 2007 in Wiley InterScience (www.interscience.wiley.com).

Preparation of hepatocyte nuclear fraction

Approximately 200 mg of liver tissues was transferred to a chilled Dounce homogenizer (Wheaton, Milliville, NJ) and homogenized on ice by 30 strokes in 1.2 mL of nuclei buffer [300 mM sucrose in 10 mM Tris-HCl, pH 7.4, 15 mM NaCl, 5 mM $MgCl_2$ and 0.25 mM phenylmethylsulfonyl fluoride (PMSF)]. The homogenate was filtered through gauze and centrifuged at 4,500*g* for 5 min at 4°C. The resulting pellet was resuspended, layered over 2 mL of nuclei buffer containing 2 M sucrose, and centrifuged at 23,000*g* for 1 hr at 4°C. The pellet obtained after ultracentrifugation was resuspended in 250 μL of nuclei buffer and used as the nuclear fraction. Preparation of nuclear fraction from isolated hepatocytes was performed as described elsewhere.[16]

Immunoblot analysis

Protein concentration was measured colorimetrically by a BCA™ Protein Assay kit (Pierce, Rockford, IL). For analysis of fatty acid-metabolizing enzymes and protein, whole liver lysate (10–20 μg protein) was subjected to 10% sodium dodecyl sulfate (SDS)-polyacrylamide gel electrophoresis.[17] For analysis of other proteins, hepatocyte nuclear fraction (100 μg protein) or whole liver lysate (200–300 μg protein) was subjected to electrophoresis. After electrophoresis, the proteins were transferred to nitrocellulose membranes, which were incubated with the primary antibody, followed by alkaline phosphatase-conjugated goat anti-rabbit or anti-mouse IgG. The origin of the primary rabbit polyclonal antibodies against fatty acid-metabolizing enzymes and protein was described earlier.[17] For immunoblot analysis of peroxisome proliferator-activated receptor α (PPARα), a polyclonal anti-mouse antibody[18] or commercial antibody (Santa Cruz Biotechnology, Santa Cruz, CA) was used. The antibodies against cell-cycle regulators and oncogene products were purchased commercially (Santa Cruz Biotech.).[19] Equal loading of the protein obtained from whole liver lysate and nuclear fraction was confirmed by reprobing the membranes with an antibody against β-actin and histone H1, respectively. The band intensity of nuclear PPARα was quantified densitometrically, normalized to that of histone H1, and subsequently expressed as the fold changes relative to that of 9-month-old nontransgenic mice.

mRNA analysis

Total liver RNA was extracted with an RNeasy Mini Kit™ (Qiagen, Valencia, CA). Five microgram of RNA was electrophoresed on 1.1 M formaldehyde-containing 1% agarose gels and transferred to nylon membranes by capillary blotting in 20× SSC buffer (3 M NaCl and 300 mM sodium citrate, pH 7.0) overnight. The membranes were hybridized with ^{32}P-labeled cDNA probes. The blots were exposed to a phosphorimager screen cassette and were analyzed using a Molecular Dynamics Storm 860 Phosphorimager system (Sunnyvale, CA). The origin of the cDNA probes has been described elsewhere.[17–19] Northern blot of β-actin was used as the internal control. The blot intensity was quantified, normalized to that of β-actin and subsequently expressed as the fold changes relative to that of 9-month-old nontransgenic mice.

Pulse-label and pulse-chase experiment

Parenchymal hepatocytes were isolated from transgenic and control mice by the modified *in situ* perfusion method.[20] After perfusion with 0.05% collagenase solution (Wako, Osaka, Japan), the isolated hepatocytes were washed thrice by means of differential centrifugation and the dead cells removed by density gradient centrifugation on Percoll (Amersham Pharmacia Biotech, Buckinghamshire, UK). The live hepatocytes were washed and suspended in William's E medium containing 5% fetal bovine serum. When the viability of the isolated hepatocytes exceeded 85% as determined by the trypan blue exclusion test, the following experiments were conducted. The isolated hepatocytes were washed twice and incubated in methionine-free medium containing 5% dialyzed fetal bovine serum for 1 hr at 37°C. The medium was replaced with the same medium containing 300 μCi/mL of [^{35}S]methionine (Amersham Pharmacia Biotech.). After 3-hr of incubation, the labeled medium was changed to the standard medium and the preparation was chased for 4, 8 or 16 hr. The labeled cells were washed, homogenized and centrifuged for preparation of the nuclear fraction. The levels of radioactivity in the homogenates of the pulse-labeled preparations were similar between the transgenic and the nontransgenic mice, suggesting that the [^{35}S]methionine uptake capacity in the former hepatocytes is similar to that in the latter. The nuclear fraction was lysed in RIPA buffer [10 mM Tris-HCl, pH 7.4, 0.2% sodium deoxycholate, 0.2% Nonidet P-40, 0.1% SDS, 0.25 mM PMSF, 10 μg/mL aprotinin]. The lysate was incubated for 3 hr at 4°C with purified anti-PPARα antibody. The immune complexes were precipitated with *Staphylococcus aureus* protein A bound to agarose beads. After the precipitates had been washed in RIPA buffer, the labeled proteins were resolved by 10% SDS-polyacrylamide gel electrophoresis and visualized by autoradiography. The nuclear fractions of the pulse-labeled preparations were also used for immunoblot analysis of PPARα.

Affinity chromatography for PPARα complex

All procedures were performed at 4°C. The nuclear fraction from the mouse liver was mixed with a 4-fold volume of a solution containing 12.5 mM potassium phosphate, pH 7.5, 25 mM NaCl, 0.25% Tween 20 and 0.1 mM PMSF. The mixture was briefly sonicated with a microsonicator, the Powersonic Model 50 (Yamato, Tokyo, Japan), and then centrifuged at 100,000*g* for 20 min. The supernatant was applied to an immobilized anti-PPARα IgG column (1.0 × 4.0 cm^2), prepared with the Affigel HZ Immunoaffinity kit^R (Bio-Rad, Hercules, CA) and equilibrated with 10 mM potassium phosphate, pH 7.5, 20 mM NaCl and 0.2% Tween 20. The solution was again passed through the column and this was repeated at least thrice. The column was washed and the elution performed with 150 mM sodium citrate, pH 3.0, and 200 mM NaCl, in a total volume of 2 mL. The eluate was resolved by 10 and 15% SDS-polyacrylamide gel electrophoresis for PPARα and the HCV core protein, respectively. The core protein expressed in COS cells was used as a positive marker.[21] The monoclonal antibody against the core protein was purchased commercially (ViroGen, Watertown, MA).

Cytochemical staining of peroxisomes

Liver peroxisome proliferation was evaluated by using 3,3′-diaminobenzidine (DAB) staining for catalase according to the method of Novikoff and Goldfischer with minor modifications.[22] Small pieces of liver were fixed with 2% glutaraldehyde in 100 mM sodium cacodylate buffer, pH 7.2, for 3 hr at 4°C, rinsed with sodium cacodylate buffer and cut into 100-μm sections with a Lancer^R Vibratome 1000 (Lancer, Bridgeton, MO). These sections were then incubated for 1 hr at 37°C in the DAB reaction medium (0.2% DAB tetrahydrochloride in 50 mM propanediol, pH 9.7, 5 mM KCN, 0.05% H_2O_2) and postfixed with 1% OsO_4 in 100 mM sodium phosphate, pH 7.4 for 1 hr. The sections were dehydrated through a graded series of ethanol and acetone treatments and embedded in Epok 812 (Oken, Tokyo, Japan). One micrometer sections were prepared, counterstained with 0.1% toluidine blue solution and examined by light microscopy. For electron microscopic examination, 0.1-μm sections were cut with a diamond knife, collected on grid meshes, stained with lead citrate and uranyl acetate and visualized with a JEM 1200EX II electron microscope (JEOL, Tokyo, Japan) at an accelerating voltage of 80 keV.

Morphometry of hepatic peroxisomes

Morphometric analysis of DAB-stained peroxisomes was carried out using electron photomicrographs. For each mouse, 10 independent fields in the pericentral area of liver lobuli were photomicrographed at an original magnification of 4,000×. At this magnification, peroxisomes smaller than 450 nm were clearly

identified. Peroxisomes were easily detected because of their high contrast because of the positive DAB reaction. In each frame, the number of peroxisomal profiles and the area of each individual profile were determined. The numerical density and volume density of peroxisomes were calculated using the following equations: numerical density (number/μm^2) = $N_P/(A_T - A_{empty})$, and volume density (%) = $A_{TP}/(A_T - A_{empty}) \times 100$, where N_P is the peroxisome number in the test area, A_T is the test area, A_{empty} is the area of the vascular and biliary lumens and that of the hepatocyte nuclei and lipid droplets, and A_{TP} is the area of total peroxisomal profiles in the test area. The area was measured with a Luzex AP image analyzer (Nireco, Tokyo, Japan).

Immunofluorescence staining

Liver samples were fixed in 4% paraformaldehyde in phosphate-buffered saline (PBS), embedded in Tissue-Tek O.C.T compound™ (Sakura Finetek, Torrance, CA) and frozen. Frozen liver 5-μm sections were prepared, washed with PBS, blocked with bovine serum albumin for 1 hr and incubated overnight with rabbit polyclonal antibodies against cyclin D1 (1:50 dilution)[19] and PPARα (1:100 dilution),[18] and with mouse monoclonal antibody against proliferating cell nuclear antigen (PCNA) (1:100 dilution).[19] After 5 washes with PBS, these sections were incubated with fluorescein isothiocyanate (FITC)-conjugated goat anti-rabbit IgG (Jackson ImmunoResearch, West Grove, PA) or donkey anti-mouse IgG (Dako). The sections were mounted and viewed with an Olympus Fluoview confocal laser scanning microscope (Olympus, Tokyo, Japan). Two-thousand hepatocyte nuclei were examined for each mouse, and the number of hepatocyte nuclei stained with the antibodies against cyclin D1, PPARα and PCNA was counted and expressed as a percentage.

Assessment of apoptotic hepatocytes

Liver samples were cut into small pieces and then fixed in 4% paraformaldehyde in PBS. These samples were dehydrated, embedded in paraffin and cut into 4-μm sections. The terminal deoxynucleotidyl transferase-mediated deoxyuridine triphosphate nick-end labeling (TUNEL) assay was performed using a MEBSTAIN Apoptosis Kit II (Medical and Biological Laboratories, Nagoya, Japan). The number of apoptotic hepatocytes in 2,000 hepatocytes was counted for each mouse, and expressed as a percentage.

Other methods

Hepatic caspase 3 activity was measured as described elsewhere.[23] For analysis of the nuclear contents of nonesterified fatty acids (NEFAs), ~150 μL of the hepatocyte nuclear fraction, containing 1–2 mg of protein, was treated with a microsonicator. Lipid extraction was performed according to a modification of the method developed by Folch *et al.*[24] and the nuclear content of NEFAs was measured with a *NEFA* C-test kit™ (Wako).

Statistical analysis

Statistical analysis was performed by means of Student's *t*-test. The results are expressed as the mean ± standard deviation. A probability value of less than 0.05 was considered to be statistically significant.

Results

Accelerated hepatocyte proliferation in HCV core gene transgenic mice

To evaluate hepatocyte proliferative activity, PCNA-positive hepatocytes were counted in male transgenic mice and nontransgenic mice. Although hepatic inflammation and hepatocyte necrosis were not detected in either group, the numbers of PCNA-positive hepatocytes were significantly increased in the 9-month-old transgenic mice compared with the 9-month-old nontransgenic mice (Fig. 1*a*). The increase was more significant in the 22-month-old transgenic mice (Fig. 1*a*). The numbers of PCNA-positive hepatocytes in the 22-month-old transgenic mice corresponded with those in HCV polyprotein-expressing transgenic mice with HCC.[25] On the other hand, the parameters of apoptosis, *i.e.*, the numbers of TUNEL-positive hepatocytes and hepatic caspase 3 activity, remained unchanged between the 2 groups at the same ages (Figs. 1*b* and 1*c*). These results suggest that spontaneous hepatocyte proliferation occurs as early as the age of 9 months and persists for a long time in HCV core gene transgenic mice.

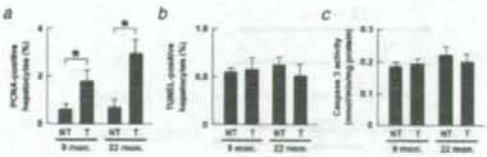

FIGURE 1 – Increase in hepatocyte proliferative activity. (*a*) The number of PCNA-positive hepatocytes. Two-thousand hepatocyte nuclei were examined for each mouse, and the number stained with anti-PCNA antibody was counted. Results are expressed as the mean ± standard deviation ($n = 8$). *, $p < 0.05$ between the transgenic mice and the nontransgenic mice; NT, nontransgenic mice; T, transgenic mice; 9 mon, 9-month-old mice; 22 mon, 22-month-old mice. (*b*) The number of apoptotic hepatocytes. The number of TUNEL-positive hepatocytes in 2,000 hepatocytes was determined for each mouse. Results are expressed as the mean ± standard deviation ($n = 8$). (*c*) Caspase 3 activity. Results are expressed as the mean ± standard deviation ($n = 8$).

Simultaneous induction of cell-cycle regulators and oncogene products in HCV core gene transgenic mouse livers

To examine the changes in the expression of proteins associated with hepatocyte division, the livers of the 9- and 22-month-old mice were subjected to immunoblot analysis. The levels of many proteins including cell-cycle regulators [cyclin-dependent kinase (CDK) 1, 2 and 4, cyclin D1 and E, and PCNA], and oncogene products (c-Myc, c-Fos and c-Ha-Ras) were significantly higher in the 22-month-old transgenic mice than in the control mice (Fig. 2). The levels of CDK inhibitors such as p16 and p21 were similar between the 2 groups. Similar results were obtained from the 9-month-old transgenic mice (data not shown). Time course changes in the expression of key G1-S checkpoint regulators, cyclin D1 and CDK4, are shown in Figure 3*a*. The simultaneous increase in the expression of cyclin D1 and CDK4 in the transgenic mice was continuous and more pronounced with age. Northern blot analysis revealed that the increase of these proteins occurred at the transcriptional level (Figs. 3*b* and 3*c*). Thus, these results reveal that various proteins which accelerate cell-cycle progression were induced simultaneously, persistently and age-dependently in the transgenic mice.

Correlative induction of PPARα targets in HCV core gene transgenic mouse livers

As shown in Figure 2, the expression of many kinds of cell-cycle regulators and oncogene products is known to be induced by the functional activation of PPARα.[19,26–30] To investigate whether PPARα is activated in the livers of transgenic mice, the expression of representative PPARα target genes,[30] acyl-CoA oxidase (AOX), peroxisomal thiolase (PT) and liver-type fatty acid-binding protein (L-FABP), was examined. As demonstrated in Figure 3*a*, the levels of AOX, PT, and L-FABP were increased in the 9-month-old transgenic mice compared with the nontransgenic mice, and the increase was more pronounced in the 22-month-old transgenic mice. Northern blot analysis demonstrated that the increase in these PPARα targets was based on the increase in the transcriptional activity (Figs. 3*b* and 3*c*). The increase in the

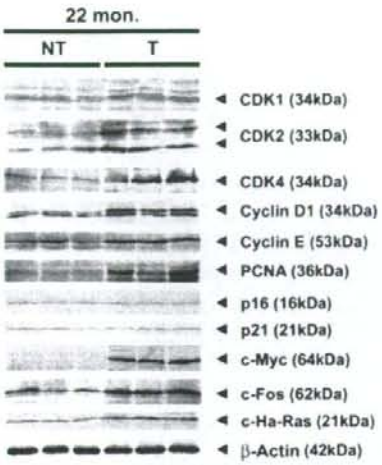

FIGURE 2 – Immunoblot analysis of cell-cycle regulators and oncogene products. Whole liver lysate (200 μg) was loaded in each lane. The band of β-actin was used as the loading control. The apparent molecular weight is indicated in parentheses. 22 mon, 22-month-old mice; NT, nontransgenic mice; T, transgenic mice.

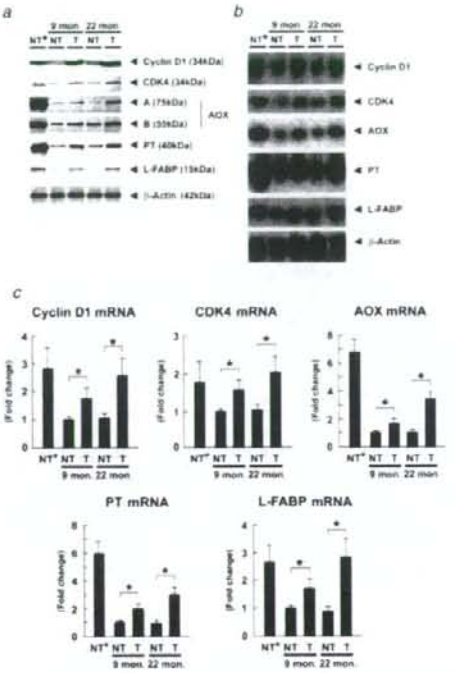

FIGURE 3 – Analysis of PPARα-regulated proteins. (*a*) Immunoblot analysis of cell-cycle regulators and fatty acid-metabolizing enzymes and proteins. Since no significant individual differences in the same mouse group were found in the preliminary experiments, 10 mg of liver pieces prepared from each mouse (n = 8/group) was mixed and homogenized. Whole liver lysate (200 μg for cyclin D1 and CDK4, and 20 μg for others) was loaded in each lane. The band of β-actin was used as the loading control. Results are representative of 4 independent experiments. The apparent molecular weight is indicated in parentheses. 9 mon, 9-month-old mice; 22 mon, 22-month-old mice; NT, nontransgenic mice; T, transgenic mice; NT*, nontransgenic mice treated with a control diet containing 0.5% clofibrate for 2 weeks; A and B, full-length and truncated AOX, respectively. (*b*) Northern blot analysis concerning the proteins in (*a*). Ten milligram of liver pieces from each mouse (n = 8/group) was mixed and homogenized, and total liver RNA was extracted. Hepatic RNA (5 μg) was separated on a denaturing gel, transferred to membranes and hybridized with the indicated ^{32}P-labeled cDNA probes. The blot of β-actin was used as the internal control. Results are representative of 4 independent experiments. (*c*) Quantification of hepatic mRNA levels. The mRNA level was quantified using a phosphorimager, normalized to that of β-actin, and subsequently normalized to that of 9-month-old nontransgenic mice. Results were obtained from 4 independent experiments and expressed as the mean ± standard deviation. Abbreviations are identical with those in (*b*). *, $p < 0.05$ between the transgenic mice and the nontransgenic mice.

mRNA expression of AOX, PT and L-FABP corresponded exactly with that of cyclin D1 or CDK4 (Figs. 3*b* and 3*c*). Therefore, these results demonstrate the strong correlation between continuous and age-dependent induction of cell-cycle regulators and functional activation of PPARα in these transgenic mice. Furthermore, the induction of these 5 proteins was also observed in wild-type mice treated with clofibrate, a potent PPARα activator; however, the degree of the induction of AOX and PT in the transgenic mice was smaller than that in the clofibrate-treated wild-type mice (Fig. 3), suggesting that the PPARα activation found in the transgenic mice was not as intense as that in the mice treated with clofibrate.

Histological evaluation of PPARα activation

An increase in the numbers of peroxisomes is associated with PPARα activation.[18] To determine whether peroxisome proliferation occurs in the HCV core gene transgenic mice, cytochemical staining for peroxisomal catalase was performed. A scattered distribution of hepatocytes with numerous peroxisomes was observed in the 9-month-old transgenic mice (Fig. 4*a*). Such hepatocytes were also found in the 22-month-old transgenic mouse livers (Fig. 4*a*). In contrast, almost all of the hepatocytes in the clofibrate-treated mice showed significant peroxisome proliferation (Fig. 4*a*). To quantitatively evaluate the degree of peroxisome proliferation, morphometric analysis of peroxisomes was conducted. The numerical density and volume density were significantly increased in the transgenic mice compared with those in the nontransgenic mice (Fig. 4*b*). The volume density, the most reliable parameter of peroxisome proliferation, was increased age-dependently in the transgenic mice, but the degree of the increase was not as prominent as that observed in mice with clofibrate administration (Fig. 4*b*). The finding that only some hepatocytes in the transgenic mice presented a marked peroxisome proliferation (Fig. 4*a*) is noteworthy, since it seems to correlate with the finding that intense expression of the core protein was observed only in particular hepatocytes.[10] These histological analyses reveal that spontaneous, continuous and age-dependent peroxisome proliferation and PPARα activation occur heterogeneously in the transgenic mouse livers, which is different from the response observed in the mice receiving clofibrate treatment.

Appearance of PPARα-, and cyclin D1-positive hepatocytes

We tried to detect abnormal hepatocytes to clarify the mechanism of hepatocarcinogenesis in the transgenic mice. On PPARα immunofluorescence staining, PPARα was primarily detected in the cytoplasm of the nontransgenic mice and the clofibrate-administered mice. Some hepatocytes having nuclei positively stained

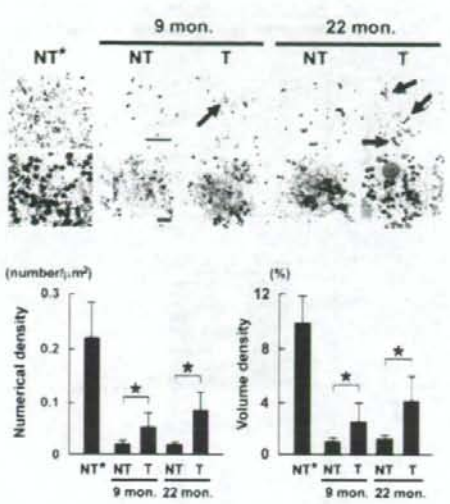

FIGURE 4 – Cytochemical staining for hepatic peroxisomes. (*a*) Light and electron photomicrographs of DAB-stained liver tissues. Peroxisomes are detected as darkly stained particles. The arrows in upper panels indicate hepatocytes showing profound peroxisome proliferation. The bars in the light and electron photomicrographs of 9-month-old nontransgenic mice indicate 50 and 2 μm, respectively. 9 mon, 9-month-old mice; 22 mon, 22-month-old mice; NT, nontransgenic mice; T, transgenic mice; NT*, nontransgenic mice treated with a control diet containing 0.5% clofibrate for 2 weeks. (*b*) Morphometric analysis of hepatic peroxisomes. The number of peroxisomes and the area of each individual peroxisome profile were measured in 10 photomicrographs for each mouse, and morphometric parameters such as numerical density and volume density were calculated. Results are expressed as the mean ± standard deviation ($n = 8$). Abbreviations are identical with those in (*a*). *, $p < 0.05$ between the transgenic mice and the nontransgenic mice.

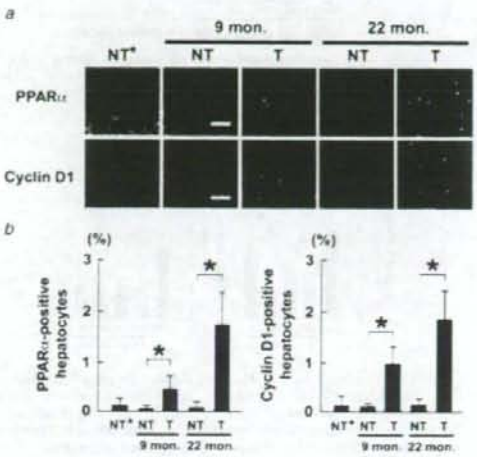

FIGURE 5 – Immunofluorescence staining for PPARα and cyclin D1. (*a*) Immunofluorescence staining using antibodies against PPARα and cyclin D1. The bars in the photomicrographs of 9-month-old nontransgenic mice indicate 50 μm. 9 mon, 9-month-old mice; 22 mon, 22-month-old mice; NT, nontransgenic mice; T, transgenic mice; NT*, nontransgenic mice treated with a control diet containing 0.5% clofibrate for 2 weeks. (*b*) The number of PPARα-, or cyclin D1-positive hepatocytes. Two-thousand hepatocyte nuclei were examined for each mouse, and the number of nuclei intensively stained with anti-PPARα or anti-cyclin D1 antibody was counted. Results are expressed as the mean ± standard deviation ($n = 8$). Abbreviations are identical with those of (*a*). *, $p < 0.05$ between the transgenic mice and the nontransgenic mice.

by anti-PPARα antibody were detected only in the transgenic mice (Fig. 5*a*). Similar to the case of PPARα, the hepatocytes having nuclei stained intensively by anti-cyclin D1 antibody were found only in the transgenic mice (Fig. 5*a*). A few hepatocytes stained by anti-CDK4 antibody were also observed only in the transgenic mice (data not shown). The frequency of appearance of PPARα-, or cyclin D1-positive hepatocytes was increased with age (Figs. 5*a* and 5*b*). Thus, the appearance of these specific hepatocytes in the transgenic mice seemed to be, at least in part, associated with sustained, age-dependent and heterogeneous PPARα activation in the transgenic mice.

Changes in PPARα levels

Since the expression of PPARα is known to be enhanced by its activation,[28,30] the quantitative change in PPARα was evaluated. The nuclear PPARα level in the transgenic mice was increased age-dependently, as expected (Figs. 6*a*, upper panel and 6*b*), but the PPARα level in the whole liver lysate remained unchanged (data not shown). The increase in nuclear PPARα in the transgenic mice was smaller than that in the clofibrate-treated wild-type mice (Figs. 6*a*, upper panel and 6*b*). Northern blot analysis revealed a higher PPARα mRNA level in the clofibrate-treated mice than in the controls, although this parameter in the transgenic mouse groups of each age was similar to that in the controls (Figs. 6*a*, lower panel and 6*b*). These results indicate that the increase in nuclear PPARα in the transgenic mice occurs mainly at the post-transcriptional level, which is distinct from that observed in the clofibrate-treated wild-type mice.

Stabilization of PPARα through a possible interaction with HCV core protein in hepatocyte nuclei

The increased stability of PPARα in hepatocyte nuclei is thought to be one of the possible causes of a disproportional increase in the nuclear PPARα level. To examine this possibility, a pulse-chase experiment was performed using isolated hepatocytes. The half-life of nuclear PPARα was ~7 hr in the control mice and 12.5 hr in the transgenic mice (Fig. 7*a*). In addition, the intensity of the labeled PPARα band (P in Fig. 7*a*, upper panels) in the control mice was similar to that in the transgenic mice. The finding that the [^{35}S]methionine uptake in the hepatocytes from the control mice was similar to that from the transgenic mice suggests that the increase in nuclear PPARα in the hepatocytes from the transgenic mice (Fig. 7*a*, lower right panel), as well as that *in vivo* (Fig. 6*a*, upper panel), is not because of the increased PPARα transfer into the nucleus.

In the transgenic mice, HCV core protein accumulated in the nuclei, as evidenced by immunoelectron microscopy,[31] suggesting a possible interaction of the core protein with PPARα in the nuclei. We therefore examined this possibility by anti-PPARα IgG affinity chromatography. When proteins combining with PPARα in hepatocyte nuclei were subjected to immunoblot analysis, the core protein was clearly detected (Fig. 7*b*). This result suggests the possibility of complex formation between the HCV core protein and PPARα, which is consistent with an interaction of the core protein with retinoid X receptor (RXR) α,[31] an essential heterodimeric partner of PPARα.[25] Thus, HCV core protein may

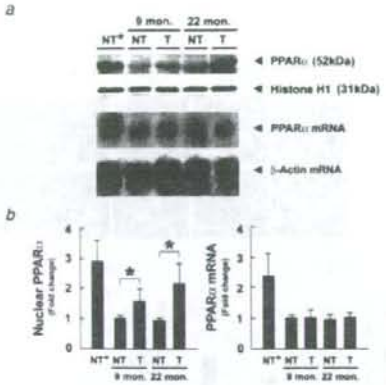

FIGURE 6 – Analysis of PPARα. (*a*) (Upper panels) Immunoblot analysis of nuclear PPARα. Since few individual differences in the same mouse group were found in the preliminary experiments, 30 mg of liver pieces from each mouse ($n = 8$/group) was mixed and homogenized to prepare the nuclear fraction. One-hundred microgram of nuclear protein was separated on 10% SDS-polyacrylamide gel, transferred to nitrocellulose membranes and reacted with antibody against PPARα. The band of histone H1 was used as the loading control. Results are representative of 4 independent experiments. The apparent molecular weight is indicated in parentheses. 9 mon, 9-month-old mice; 22 mon, 22-month-old mice; NT, nontransgenic mice; T, transgenic mice; NT*, nontransgenic mice treated with a control diet containing 0.5% clofibrate for 2 weeks. (Lower panels) Northern blot analysis of PPARα. A sample used in Figure 3*b* was adopted. Hepatic RNA (5 μg) was electrophoresed and hybridized with cDNAs for PPARα and β-actin, respectively. Results are representative of 4 independent experiments. (*b*) Quantification of nuclear PPARα levels and PPARα mRNA levels. The nuclear PPARα level was quantified densitometrically and normalized to the histone H1 level. The mRNA level of PPARα was quantified using a phosphorimager and normalized to that of β-actin. Values were subsequently normalized to those of 9-month-old nontransgenic mice. Results were obtained from 4 independent experiments and expressed as the mean ± standard deviation. Abbreviations are identical with those in (*a*). *, $p < 0.05$ between the transgenic mice and the nontransgenic mice.

directly or indirectly affect the stability of PPARα in hepatocyte nuclei.

Increase in PPARα ligands

PPARα is a ligand-activated transcription factor. Since the transgenic mice were fed a standard laboratory chow, endogenous substances such as NEFAs would serve as ligands of PPARα[33]; therefore, the contents of NEFAs in hepatocyte nuclei were compared between the 2 groups. The levels of NEFAs in hepatocyte nuclei in the transgenic mice were ~5 times higher than those in the control mice at the same age (Fig. 7*c*). This could account for the higher activation of PPARα in the transgenic mice than in the controls.

Discussion

A large number of variables are involved in the induction of HCC by HCV core protein. While the precise mechanism underlying hepatocarcinogenesis in HCV core gene transgenic mice cannot be fully elucidated from this study, our results could provide some clues to explain this phenomenon. We found spontaneous, persistent, age-dependent and heterogeneous PPARα activation in the transgenic mouse livers for the first time. This study thus advances our understanding of the association

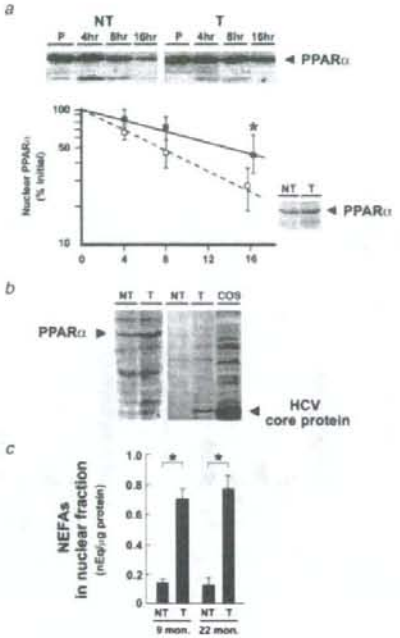

FIGURE 7 – Analyses of PPARα stability, interaction between PPARα with the core protein in hepatocyte nuclei, and nuclear contents of NEFAs. (*a*) Pulse-label and pulse-chase experiments for nuclear PPARα using isolated mouse hepatocytes. (Upper panels) Labeled PPARα bands on X-ray film. Pulse-label and pulse-chase experiments were performed as described in the Material and methods. NT, nontransgenic mice; T, transgenic mice; P, pulse-label; 4, 8, 16 hr, pulse-chase for 4, 8, 16 hr, respectively. (Lower left panel) Intensity plot of PPARα in 5 independent experiments. Values are normalized as a percentage of the values of the pulse-labeled band and expressed as the mean ± standard deviation. Open square, nontransgenic mice; black square, transgenic mice; *, $p < 0.05$ between the transgenic mice and the nontransgenic mice. (Lower right panel) Immunoblot analysis of an isolated hepatocyte nuclear fraction. NT, nontransgenic mice; T, transgenic mice. (*b*) Interaction between PPARα and HCV core protein in the nucleus. (Left panel) Immunoblot analysis (PPARα) of the eluate on anti-PPARα IgG affinity column chromatography. (Right panel) Immunoblot analysis (HCV core protein) of the same eluate. NT, nontransgenic mice; T, transgenic mice; COS, HCV core protein-overexpressing COS cell lysate. (*c*) Nuclear contents of NEFAs. The levels of NEFAs were measured using a hepatocyte nuclear fraction. Results are expressed as the mean ± standard deviation ($n = 8$). *, $p < 0.05$ between the transgenic mice and the nontransgenic mice; NT, nontransgenic mice; T, transgenic mice; 9 mon, 9-month-old mice; 22 mon, 22-month-old mice.

between HCV core protein-mediated hepatocarcinogenesis and persistent PPARα activation.

Hepatocyte proliferation is influenced by various factors, such as mitogenic chemicals, cytokines, growth factors and transcription factors. It has been reported that various kinds of cell-cycle regulators and oncogene products are induced by PPARα activation.[19,26–30] In particular, cyclin D1, CDK4, PCNA and c-Myc are potent and critical regulators of the G1-S checkpoint and cell-cycle progression,[13,14] and aberrant expression of these proteins is frequently detected in HCV-related HCC.[34–37] These key regulators are known to be induced in a PPARα-dependent manner in mice[19,30]; the continuous induction of these proteins and the

resultant acceleration of hepatocyte proliferation found in the transgenic mice may be attributed to persistent PPARα activation. In the current study, we demonstrated that there was a great variety of the intensity of PPARα activation among different hepatocytes (Fig. 4). This persistent and heterogeneous PPARα activation found especially in the transgenic mice may be linked with the age-dependent and multicentric hepatocarcinogenesis induced by the core protein.

It is well-known that the long-term administration of potent peroxisome proliferators such as fibrate drugs can induce hepatocarcinogenesis in rodents.[29] The findings observed in the transgenic mice markedly differ from those in mice with long-term treatment of peroxisome proliferators in several ways. Namely, the transgenic mice show no intense increase in AOX and PT (Fig. 3), no increase in PPARα mRNA (Fig. 6), heterogeneous peroxisome proliferation (Fig. 4) and age-dependent emergence of hepatocytes having nuclei stained intensively by anti-PPARα or anti-cyclin D1 antibody (Fig. 5). Therefore, the mode of PPARα activation and the mechanism of hepatocarcinogenesis caused by HCV core protein expression are indeed unique.

One of the mechanisms involved in the core protein-specific PPARα activation in mice is stabilization of PPARα in hepatocyte nuclei through a possible interaction with the core protein. In cultured cells expressing the core protein, it has been demonstrated that the core protein interacts with the PPARα-RXRα heterodimer and enhances the transcriptional activation mediated by PPARα regardless of the presence or absence of its ligands.[31] Since PPARα is ubiquitinated and degraded *via* the proteasome pathway,[38] it may be postulated that HCV core protein directly or indirectly influences the degradation pathway. It has been reported that the core protein binds to the proteasome activator PA28γ[39] which is known to combine with steroid receptor coactivator-3 and to accelerate its degradation.[40] Another possible mechanism is an increase in NEFAs in hepatocyte nuclei. The PPARα activation induced by the core protein enhances the expression of L-FABP,[30] which serves as a transporter of NEFAs into nuclei. Indeed, real-time confocal and multiphoton laser scanning microscopy has shown that L-FABP expression significantly increased the total uptake of medium- and long-chain fluorescent fatty acids into the nuclei of living cells.[41] Thus, increased L-FABP expression may facilitate the shuttling of NEFAs into hepatocyte nuclei for donating NEFAs to PPARα, leading to PPARα activation and further increase in L-FABP expression. Moreover, the binding of ligands causes conformational alternation of PPARα[42] and further stabilizes it in nuclei,[32] resulting in synergistic PPARα activation. Therefore, these findings concerning spontaneous and persistent PPARα activation induced by the core protein enable us to partially explain the precise molecular mechanism of hepatocarcinogenesis in HCV core gene transgenic mice.

The results obtained from the current study are consistent with the findings observed in chronically HCV-infected patients in several ways. That is, like the transgenic mice in the present study, chronically HCV-infected patients have been reported to show accelerated hepatocyte proliferation,[43] an increase in CDK4, cyclin D1 and E, PCNA, c-Myc and c-Fos,[34–37] and multicentric appearance of HCC.[44] Furthermore, it has been reported that a massive proliferation of peroxisomes was found in human non-tumorous liver tissue adjacent to HCC.[45] Thus the earlier findings, including the unique function of HCV core protein *in vivo* and the diverse and significant roles of PPARα, may help to partially understand the onset and development of HCC in patients with chronic HCV infection. It has been demonstrated that the function of hepatic PPARα was impaired in patients with chronic HCV infection,[46] which is different from our results. Since HCC had not yet developed in the patients in the report, this discrepancy might derive from differences in the stage of the hepatocarcinogenic process.

The interpretation based on persistent activation of PPARα pertains to only one possible mechanism of hepatocarcinogenesis induced by the effects of HCV core protein. We cannot rule out the presence of other mechanisms. The exact relationship between PPARα activation and hepatocarcinogenesis may be elucidated by additional experiments in which PPARα activation is continuously inhibited in the same transgenic mice. Furthermore, the exact relationship may be confirmed when PPARα-null mice bearing the core protein gene do not represent development of HCC.

In conclusion, we demonstrated for the first time that spontaneous, persistent, age-dependent and heterogeneous activation of PPARα occurred in HCV core protein transgenic mice and caused continuous enhancement of hepatocyte proliferation, which may have contributed to the age-dependent and multicentric hepatocarcinogenesis observed in these mice. In addition, we observed nuclear stabilization of PPARα and an increase in NEFAs in the hepatocyte nuclei of the transgenic mice, which may have resulted in the HCV core protein-specific PPARα activation.

References

1. Kiyosawa K, Tanaka E, Sodeyama T. Hepatitis C virus and hepatocellular carcinoma. In: Reesink HW, ed. Hepatitis C virus: Current Studies in Hematology & Blood Transfusion, vol. 62. Basel: Karger, 1998.161–180.
2. Saito I, Miyamura T, Ohbayashi A, Harada H, Katayama T, Kikuchi S, Watanabe Y, Koi S, Onji M, Ohta Y, Choo QL, Houghton M, et al. Hepatitis C virus infection is associated with the development of hepatocellular carcinoma. Proc Natl Acad Sci USA 1990;87:6547–49.
3. Tanaka Y, Hanada K, Mizokami M, Yeo AE, Shih JW, Gojobori T, Alter HJ. A comparison of the molecular clock of hepatitis C virus in the United States and Japan predicts that hepatocellular carcinoma incidence in the United States will increase over the next two decades. Proc Natl Acad Sci USA 2002;99:15584–89.
4. Kiyosawa K, Umemura T, Ichijo T, Matsumoto A, Yoshizawa K, Gad A, Tanaka E. Hepatocellular carcinoma: recent trends in Japan. Gastroenterology 2004;127:S17–S26.
5. Watashi K, Shimotohno K. The roles of hepatitis C virus proteins in modulation of cellular functions: a novel action mechanism of the HCV core protein on gene regulation by nuclear hormone receptors. Cancer Sci 2003;94:937–43.
6. Ray RB, Lagging LM, Meyer K, Ray R. Hepatitis C virus core protein cooperates with *ras* and transforms primary rat embryo fibroblasts to tumorigenic phenotype. J Virol 1996;70:4438–43.
7. Ray RB, Meyer K, Ray R. Suppression of apoptotic cell death by hepatitis C virus core protein. Virology 1996;226:176–82.
8. McLauchlan J. Properties of the hepatitis C virus core protein: a structural protein that modulates cellular processes. J Viral Hepat 2000; 7:2–14.
9. Tellinghuisen TL, Rice CM. Interaction between hepatitis C virus proteins and host cell factors. Curr Opin Microbiol 2002;5:419–27.
10. Moriya K, Yotsuyanagi H, Shintani Y, Fujie H, Ishibashi K, Matsuura Y, Miyamura T, Koike K. Hepatitis C virus core protein induces hepatic steatosis in transgenic mice. J Gen Virol 1997;78:1527–31.
11. Moriya K, Fujie H, Shintani Y, Yotsuyanagi H, Tsutsumi T, Ishibashi K, Matsuura Y, Kimura S, Miyamura T, Koike K. The core protein of hepatitis C virus induces hepatocellular carcinoma in transgenic mice. Nat Med 1998;4:1065–7.
12. Moriya K, Nakagawa K, Santa T, Shintani Y, Fujie H, Miyoshi H, Tsutsumi T, Miyazawa T, Ishibashi K, Horie T, Imai K, Todoroki T, et al. Oxidative stress in the absence of inflammation in a mouse model for hepatitis C virus-associated hepatocarcinogenesis. Cancer Res 2001;61:4365–70.
13. Sherr CJ. Cancer cell cycles. Science 1996;274:1672–7.
14. Vousden KH, Evan GI. Proliferation, cell cycle and apoptosis in cancer. Nature 2001;411:342–8.
15. Donato MF, Arosio E, Del Ninno E, Ronchi G, Lampertico P, Morabito A, Balestrieri MR, Colombo M. High rates of hepatocellular carcinoma in cirrhotic patients with high liver cell proliferative activity. Hepatology 2001;34:523–8.
16. Yasui K, Wakita T, Tsukiyama-Kohara K, Funahashi S-I, Ichikawa M, Kajita T, Moradpour D, Wands JR, Kohara M. The native form and maturation process of hepatitis C virus core protein. J Virol 1998;72:6048–55.
17. Aoyama T, Peters JM, Iritani N, Nakajima T, Furihata K, Hashimoto T, Gonzalez FJ. Altered constitutive expression of fatty acid-metabo-

lizing enzymes in mice lacking the peroxisome proliferator-activated receptor α (PPARα). J Biol Chem 1998;273:5678–84.
18. Lee SS, Pineau T, Drago J, Lee EJ, Owens JW, Kroetz DL, Fernandez-Salguero PM, Westphal H, Gonzalez FJ. Targeted disruption of the α isoform of the peroxisome proliferator-activated receptor gene in mice results in abolishment of the pleiotropic effects of peroxisome proliferators. Mol Cell Biol 1995;15:3012–22.
19. Peters JM, Aoyama T, Cattley RC, Nobumitsu U, Hashimoto T, Gonzalez FJ. Role of peroxisome proliferator-activated receptor α in altered cell cycle regulation in mouse liver. Carcinogenesis 1998; 19:1989–94.
20. Ni R, Tomita Y, Matsuda K, Ichihara A, Ishimura K, Ogasawara J, Nagata S. Fas-mediated apoptosis in primary cultured mouse hepatocytes. Exp Cell Res 1994;215:332–7.
21. Harada S, Watanabe Y, Takeuchi K, Suzuki T, Katayama T, Takebe Y, Saito I, Miyamura T. Expression of processed core protein of hepatitis C virus in mammalian cells. J Virol 1991;65:3015–21.
22. Novikoff AB, Goldfischer S. Visualization of peroxisomes (microbodies) and mitochondria with diaminobenzidine. J Histochem Cytochem 1969;17:675–80.
23. Gurtu V, Kain SR, Zhang G. Fluorometric and colorimetric detection of caspase activity associated with apoptosis. Anal Biochem 1997; 251:98–102.
24. Folch J, Lees M, Sloane Stanley GH. A simple method for the isolation and purification of total lipids from animal tissues. J Biol Chem 1957;226:497–509.
25. Furutani T, Hino K, Okuda M, Gondo T, Nishina S, Kitase A, Korenaga M, Xiao SY, Weinman SA, Lemon SM, Sakaida I, Okita K. Hepatic iron overload induces hepatocellular carcinoma in transgenic mice expressing the hepatitis C virus polyprotein. Gastroenterology 2006;130:2087–98.
26. Cherkaoui-Malki M, Lone YC, Corral-Debrinski M, Latruffe N. Differential proto-oncogene mRNA induction from rats treated with peroxisome proliferators. Biochem Biophys Res Commun 1990; 173:855–61.
27. Ledwith BJ, Johnson TE, Wagner LK, Pauley CJ, Manam S, Galloway SM, Nichols WW. Growth regulation by peroxisome proliferators: opposing activities in early and late G1. Cancer Res 1996; 56:3257–64.
28. Rininger JA, Goldsworthy TL, Babishi JG. Time course comparison of cell-cycle protein expression following partial hepatectomy and WY14,643-induced hepatic cell proliferation in F344 rats. Carcinogenesis 1997;18:935–41.
29. Peters JM, Cheung C, Gonzalez FJ. Peroxisome proliferator-activated receptor-α and liver cancer: where do we stand? J Mol Med 2005; 83:774–85.
30. Mandard S, Muller M, Kersten S. Peroxisome proliferator-activated receptor α target genes. Cell Mol Life Sci 2004;61:393–416.
31. Tsutsumi T, Suzuki T, Shimoike T, Suzuki R, Moriya K, Shintani Y, Fujie H, Matsuura Y, Koike K, Miyamura T. Interacton of hepatitis C virus core protein with retinoid X receptor α modulates its transcriptional activity. Hepatology 2002;35:937–46.
32. Tanaka N, Hora K, Makishima H, Kamijo Y, Kiyosawa K, Gonzalez FJ, Aoyama T. In vivo stabilization of nuclear retinoid X receptor α in the presence of peroxisome proliferator-activated receptor α. FEBS Lett 2003;543:120–4.
33. Desvergne B, Wahli W. Peroxisome proliferator-activated receptors: nuclear control of metabolism. Endocr Rev 1999;20:649–88.
34. Ito Y, Sasaki Y, Horimoto M, Wada S, Tanaka Y, Kasahara A, Ueki T, Hirano T, Yamamoto H, Fujimoto J, Okamoto E, Hayashi N, et al. Activation of mitogen-activated protein kinases/extracellular signal-regulated kinases in human hepatocellular carcinoma. Hepatology 1998;27:951–8.
35. Masahi T, Shiratori Y, Rengifo W, Igarashi K, Yamagata M, Kurokohchi K, Uchida N, Miyauchi Y, Yoshiji H, Watanabe S, Omata M, Kuriyama S. Cyclins and cyclin-dependent kinases: comparative study of hepatocellular carcinoma versus cirrhosis. Hepatology 2003;37:534–43.
36. Nardone G, Romano M, Calabro A, Pedone PV, de Sio I, Persico M, Budillon G, Bruni CB, Riccio A, Zarrilli R. Activation of fetal promoters of insulin-like growth factors II gene in hepatitis C virus-related chronic hepatitis, cirrhosis, and hepatocellular carcinoma. Hepatology 1996;23:1304–12.
37. Kawate S, Fukusato T, Ohwada S, Watanuki A, Morishita Y. Amplification of *c-myc* in hepatocellular carcinoma: correlation with clinicopathologic features, proliferative activity and p53 overexpression. Oncology 1999;57:157–63.
38. Genini D, Catapano CV. Control of peroxisome proliferator-activated receptor fate by the ubiquitin-proteasome system. J Recept Signal Transduct Res 2006;26:679–92.
39. Moriishi K Okabayashi T, Nakai K, Moriya K, Koike K, Murata S, Chiba T, Tanaka K, Suzuki R, Suzuki T, Miyamura T, Matsuura Y. Proteasome activator PA28γ-dependent nuclear retention and degradation of hepatitis C virus core protein. J Virol 2003;77:10237–49.
40. Li X, Lonard D, Jung SY, Malovannaya A, Feng Q, Qin J, Tsai SY, Tsai M, O'Malley BW. The SRC-3/AIB1 coactivator is degraded in a ubiquitin- and ATP-independent manner by the REGγ proteasome. Cell 2006;124:381–92.
41. Huang H, Starodub O, McIntosh A, Kier AB, Schroeder F. Liver fatty acid-binding protein targets fatty acids to the nucleus. Real time confocal and multiphoton fluorescence imaging in living cells. J Biol Chem 2002;277:29139–51.
42. Dowell P, Peterson VJ, Zabriskie TM, Leid M. Ligand-induced peroxisome proliferator-activated receptor α conformational change. J Biol Chem 1997;272:2013–20.
43. Farinati F, Cardin R, Fiorentino M, D'Errico A, Grigioni W, Cecchetto A, Naccarato R. Imbalance between cytoproliferation and apoptosis in hepatitis C virus related chronic liver disease. J Viral Hepat 2001;8:34–40.
44. Oikawa T, Ojima H, Yamasaki S, Takayama T, Hirohashi S, Sakamoto M. Multistep and multicentric development of hepatocellular carcinoma: histological analysis of 980 resected nodules. J Hepatol 2005;42:225–9.
45. Litwin JA, Beier K, Volkl A, Hofmann WJ, Fahimi HD. Immunocytochemical investigation of catalase and peroxisomal lipid β-oxidation enzymes in human hepatocellular tumors and liver cirrhosis. Virchows Arch 1999;435:486–95.
46. Dharancy S, Malapel M, Perlemuter G, Roskams T, Cheng Y, Dubuquoy L, Podevin P, Conti F, Canva V, Philippe D, Gambiez L, Mathurin P, et al. Impaired expression of the peroxisome proliferator-activated receptor α during hepatitis C virus infection. Gastroenterology 2005;128:334–2.

J Gastroenterol 2009; 44[Suppl XIX]:82–88
DOI 10.1007/s00535-008-2276-4

Journal of Gastroenterology

Steatosis, liver injury, and hepatocarcinogenesis in hepatitis C viral infection

KAZUHIKO KOIKE

Department of Infectious Diseases, Internal Medicine, Graduate School of Medicine, University of Tokyo, 7-3-1 Hongo, Bunkyo-ku, Tokyo 113-8655, Japan

In addition to the link with development of hepatocellular carcinoma (HCC), hepatitis C virus (HCV) infection is associated with several hepatic and extrahepatic manifestations. A role of hepatic steatosis in the pathogenesis of chronic hepatitis C has been shown, implying hepatitis C as a metabolic disease. Furthermore, recent epidemiological studies have suggested a linkage between insulin resistance and chronic HCV infection. In addition to the data indicating the presence of lipid metabolism disturbance and insulin resistance in the cohort of chronic hepatitis C patients, we found evidence showing the association between these two conditions and HCV infection using mice transgenic for the HCV core gene. These mice develop HCC late in life after the phase of hepatic steatosis and insulin resistance. The nonappearance of both steatosis and HCC in HCV core gene transgenic mice that are null for the proteasome activator 28γ implies a close relationship between lipid metabolism disturbance and hepatocarcinogenesis. Also, the core protein is shown to bind with retinoid X receptor (RXR)-α, resulting in the upregulation of some lipid metabolism enzymes, including cellular retinol binding protein II and acyl-CoA oxidase. In addition, the persistent activation of peroxisome proliferator activated receptor (PPAR)-α has recently been found in the liver of HCV core gene transgenic mice, yielding dramatic changes in lipid metabolism and hepatocyte proliferation, including HCC development. These results would provide a clue for further understanding of the role of lipid metabolism in pathogenesis of HCV infection, including liver injury and hepatocarcinogenesis.

Received: June 9, 2008 / Accepted: August 10, 2008
Reprint requests to: K. Koike

Key words: lipid metabolism, transgenic mouse, oxidative stress, intracellular signal transduction, peroxisome proliferator activated receptor

Introduction

Worldwide, approximately 170 million people are persistently infected with hepatitis C virus (HCV), which induces a spectrum of chronic liver diseases from chronic hepatitis to cirrhosis and, eventually, to hepatocellular carcinoma (HCC).[1] HCV has been given increasing attention because of its wide and deep penetration in the community, tied with a very high incidence of HCC in persistent HCV infection. Once liver cirrhosis is established in hosts persistently infected with HCV, HCC develops at a yearly rate of approximately 7%,[2] resulting in the development of HCC in nearly 90% of HCV-associated cirrhotic patients in 15 years. In addition, the outstanding features in the mode of hepatocarcinogenesis in HCV infection, i.e., development of HCC in a multicentric fashion and at a very high incidence, are not common in other malignancies except for hereditary cancers such as familial polyposis of the colon. Knowledge of the mechanism underlying HCC development in persistent HCV infection, therefore, is imminently required for the prevention of HCC.

In addition to the link with development of HCC, HCV infection is associated with several hepatic and extrahepatic manifestations.[3] A role of hepatic steatosis in the pathogenesis of chronic hepatitis C has been shown, implicating hepatitis C as a metabolic disease.[4] Moreover, recent epidemiological studies have suggested a linkage between insulin resistance and chronic HCV infection.[5] In addition to the epidemiological data indicating the presence of lipid metabolism disturbance and insulin resistance in the cohort of chronic hepatitis C patients, detailed analyses on the relationship between

metabolic disorders and chronic hepatitis C have revealed evidence showing a close association between the progression of liver fibrosis and metabolic abnormalities in HCV infection.[6] However, it is unclear yet whether a causative relationship exists between these medical conditions. Moreover, it is unclear whether such metabolic disorders contribute to hepatocarcinogenesis in HCV infection.

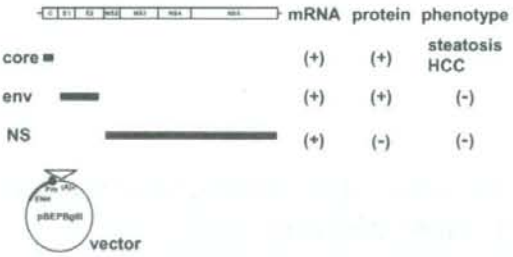

Fig. 1. Transgenic mouse lines carrying the hepatitis C virus (HCV) genome. Three different kinds of transgenic mouse lines, carrying the *core* gene, envelope genes, or nonstructural genes of HCV, respectively, were established under the control of the same regulatory elements. Among these mouse strains, only the transgenic mice carrying the HCV core gene develop hepatocellular carcinoma (HCC) after an early phase with hepatic steatosis in two independent lineages. The mice transgenic for the envelope genes or nonstructural genes do not develop HCC. *HCC*, hepatocellular carcinoma; *env*, envelope genes; *NS*, nonstructural genes

Possible roles of HCV in hepatocarcinogenesis

The mechanism underlying hepatocarcinogenesis in HCV infection is not yet fully understood, despite the fact that nearly 80% of patients with HCC in Japan are persistently infected with HCV.[1,7,8] HCV infection is also common in patients with HCC in other countries, albeit to a lesser extent. These lines of evidence prompted us to seek to determine the role of HCV in hepatocarcinogenesis. Inflammation induced by HCV should be considered, of course, in a study on the hepatocarcinogenesis in hepatitis viral infection: necrosis of hepatocytes caused by chronic inflammation followed by regeneration enhances genetic aberrations in host cells, the accumulation of which culminates in HCC. This theory presupposes an indirect involvement of hepatitis viruses in HCC via hepatic inflammation. However, this context leaves us with a serious question: can inflammation alone result in the development of HCC in such a high incidence (90% in 15 years) or multicentric nature in HCV infection?

The other role of HCV would have to be weighed against an extremely rare occurrence of HCC in patients with autoimmune hepatitis in which severe inflammation in the liver persists indefinitely, even after the development of cirrhosis. This background and reasoning lead to a possible activity of viral proteins for inducing neoplasia. This possibility has been evaluated by introducing genes of HCV into hepatocytes in culture with little success. One of the difficulties in using cultured cells is the carcinogenic capacity of HCV, if any, which would be weak and would take a long time to manifest. Actually, it takes 30–40 years for HCC to develop in individuals infected with HCV. On the basis of these points of view, we started to investigate carcinogenesis in chronic hepatitis C, in vivo, by transgenic mouse technology.

HCV core protein has an in vivo oncogenic activity as revealed by animal studies

Transgenic mouse lines carrying the HCV genome were engineered by introducing the genes from the cDNA of the HCV genome of genotype 1b.[9,10] Established are three different kinds of transgenic mouse lines, which carry the core gene, envelope genes, or nonstructural genes, respectively, under the same transcriptional regulatory element. Among these mouse lines, only the transgenic mice carrying the core gene developed HCC in two independent lineages.[10] The envelope gene transgenic mice do not develop HCC, despite high expression levels of both E1 and E2 proteins,[11,12] and the transgenic mice carrying the entire nonstructural genes have developed no HCC (Fig. 1).

The core gene transgenic mice express the core protein of an expected size, and the level of the core protein in the liver is similar to that in chronic hepatitis C patients. Early in life, these mice develop hepatic steatosis, which is one of the histological characteristics of chronic hepatitis C, along with lymphoid follicle formation and bile duct damage.[13] Thus, the core gene transgenic mouse model reproduces well the features of chronic hepatitis C. Of note, no pictures of significant inflammation are observed in the liver of this animal model. Late in life, these transgenic mice develop HCC. Notably, the development of steatosis and HCC has been reproduced by other HCV transgenic mouse lines, which harbor the entire HCV genome or structural genes including the core gene.[14–16] These outcomes indicate that the core protein, per se, of HCV has an oncogenic potential when expressed in vivo.

Oxidative stress overproduction and intracellular signaling pathway activation are the major pathways in the core-induced liver pathology

It is difficult to elucidate the mechanism underlying the development of HCC, even for our simple model in which only the core protein is expressed in otherwise normal liver. There is a notable feature in the localization of the core protein in hepatocytes; while the core protein predominantly exists in the cytoplasm associated with lipid droplets, it is also present in the mitochondria and nuclei.[10,17] On the basis of this finding, the pathways related to these two organelles, the mitochondria and nuclei, were thoroughly investigated.

One effect of the core protein is an increased production of oxidative stress in the liver. We would like to draw particular attention to the fact that the production of oxidative stress is increased in our transgenic mouse model in the absence of inflammation in the liver. This finding reflects a state of overproduction of reactive oxygen species (ROS) in the liver,[18] or predisposition to it, which is staged by the HCV core protein without any intervening inflammation.[19,20] The overproduction of oxidative stress results in the generation of deletions in mitochondrial and nuclear DNA, an indicator of genetic damage. In addition, analysis of antioxidant system revealed that some antioxidative molecules are not increased despite the overproduction of ROS in the liver of core gene transgenic mice: hemeoxygenase-1 and glutathione peroxidase are not augmented whereas catalase and glutathione S-transferase levels are increased and enhanced by iron overloading (Moriya et al., manuscript in preparation). These results suggest that HCV core protein not only induces overproduction of ROS but also attenuates some of the antioxidant systems, which may explain the mechanism underlying the production of a strong oxidative stress in HCV infection compared to other forms of hepatitis.

In the absence of inflammation, thus, the core protein induces oxidative stress overproduction, which may, at least in part, contribute to hepatocarcinogenesis in HCV infection. If inflammation were added to the liver with the HCV core protein, the production of oxidative stress would be escalated to an extent that can no longer be scavenged by a physiological antagonistic system. This idea suggests that the inflammation in chronic HCV infection would have a characteristic difference in its quality from those of other types of hepatitis, such as autoimmune hepatitis. The basis for the overproduction of oxidative stress may be ascribed to the mitochondrial dysfunction.[10,19] The dysfunction of the electron transfer system of the mitochondrion is suggested in association with the presence of the HCV core protein.[21]

Other pathways in hepatocarcinogenesis would be the alteration of the expression of cellular genes and modulation of intracellular signaling pathways. For example, tumor necrosis factor (TNF)-α and interleukin-1β have been found to be transcriptionally activated.[22] The mitogen-activated protein kinase (MAPK) cascade is also activated in the liver of the core gene transgenic mouse model. The MAPK pathway, which consists of three routes, c-Jun N-terminal kinase (JNK), p38, and extracellular signal-regulated kinase (ERK), is involved in numerous cellular events including cell proliferation. In the liver of the core gene transgenic mouse model before HCC development, only the JNK route is activated. Downstream of JNK activation, transcription factor activating protein (AP)-1 activation is markedly enhanced.[20,21] At far downstream, both the mRNA and protein levels of cyclin D1 and CDK4 are increased. Thus, the HCV core protein modulates the intracellular signaling pathways and gives an advantage for cell proliferation to the hepatocytes. Interestingly, we found recently that a protein interacting with the core protein, proteasome activator 28γ (PA28γ), is indispensable for the core protein to exert its function for the development of steatosis, insulin resistance, and HCC.[23,24]

Lipid metabolism and HCV infection

Steatosis is frequently observed in chronic hepatitis C patients and is significantly associated with increased fibrosis and progression rate of fibrosis of the liver.[6] A comprehensive analysis of gene expression in the liver of core gene transgenic mice, in which steatosis develops from early in life, revealed that a number of genes related to lipid metabolism are significantly upregulated or downregulated (Table 1).

The composition of fatty acids that are accumulated in the liver of core gene transgenic mice is different from that in fatty liver resulting from simple obesity. Carbon-18 monounsaturated fatty acids (C18:1) such as oleic or vaccenic acids are significantly increased; this is also the case in the comparison of liver tissues from hepatitis C patients and patients with simple fatty liver due to obesity.[20] The mechanism of steatogenesis in hepatitis C was investigated using this mouse model. There are at least three pathways for the development of steatosis. One is the frequent presence of insulin resistance in hepatitis C patients as well as in the core gene transgenic mice, which occurs through the inhibition of tyrosine phosphorylation of insulin receptor substrate (IRS)-1.[25] Insulin resistance increases the peripheral release and hepatic uptake of fatty acids, resulting in an accumulation of lipid in the liver. The second pathway is the suppression of the activity of

Table 1. Cellular genes differentially expressed in hepatitis C virus (HCV) core transgenic mouse liver

	Upregulated	Downregulated
Lipid metabolism	NPC1 Catalase Very long chain acyl-CoA dehydrogenase Carboxylesterase selenoprotein P Carbonic anhydrase Adipose differentiation-related protein Bilirubin/phenol family UDP glucuronosyltransferase	Stearoyl-CoA desaturase Sterol-carrier protein X Alpha-enolase carnitine acetyltransferase Gal beta 1,4(3) GlcNAc alpha 2,3-sialyltransferase Very long chain acyl-CoA synthetase Liver transferrin 4-Hydroxyphenylpyruvate dioxygenase LAF1 transketolase *s*-Adenosylmethionine synthetase Apolipoprotein A-II
Transcription and cell proliferation	Int-6 GCN5L1 *H. sapiens* 8.2k-Da differentiation factor USF1 Initiation factor eIF-4AI Human elongation factor-1-delta Sui1	Human guanine nucleotide regulatory protein Alpha-fetoprotein Retinol binding protein
Inflammation	Alpha-1 protease inhibitor 3 Hemopexin	Alpha-2-macroglobulin LMW prekininogen Complement component C3 AHSG(alpha 2 HS-glycoprotein) homologue
Others	Microvascular endothelial differentiation gene 1 Diazepam-binding inhibitor Argininosuccinate synthetase Skeletal muscle alpha-tropomyosin Ampd3 gene DNA-binding protein	Vitronectin Epithelin 1 and 2 Murinoglobulin

microsomal triglyceride transfer protein (MTP) by HCV core protein[26]; this inhibits the secretion of very low density protein (VLDL) from the liver, yielding an increase of triglycerides in the liver. The last pathway involves sterol regulatory element-binding protein (SREBP)-1c, which regulates the production of triglycerides and phospholipids. In HCV core gene transgenic mice, SREBP-1c is activated, whereas neither SREBP-2 nor SREBP-1a is upregulated.[27]

In relation to lipid metabolism, the core protein has also been found to interact with retinoid X receptor (RXR)-α.[28] RXR-α is one of the nuclear receptors, which forms a homodimer or heterodimers with other nuclear receptors, including PPAR (peroxisome proliferator-activated receptor)-α, and plays a pivotal role in the regulation of the expression of genes relating to lipid metabolism, cell differentiation, and proliferation. In fact, the core protein of HCV activates genes that have an RXR-α-responsive element as well as those with a PPAR-α-responsive element, both in mice and in cultured cells.[28] Based on these results, we, then, examined the expression and function of PPAR-α in the liver of core gene transgenic mice.

PPAR-α activation in HCV-associated hepatocarcinogenesis

PPAR-α, one of the PPAR genes, plays a central role as a heterodimer with RXR-α in regulating fatty acid transport and catabolism. It is also known as a molecular target for lipid-lowering fibrate drugs.[29] On the other hand, prolonged administration of PPAR-α agonists causes HCC in rodents. Currently, there is little evidence that the low-affinity fibrate ligands are associated with human cancers, but it is possible that chronic activation of high-affinity ligands could be carcinogenic in humans.[29]

The level of PPAR-α protein was increased in the liver of core gene transgenic mice as early as 9 months of age. PPAR-α protein is accumulated with age in the nuclei of hepatocytes together with cyclin D1 protein. However, the level of PPAR-α mRNA was not increased at any age. By pulse-chase experiment, the stability of nuclear PPAR-α was increased in the presence of the core protein. In line with the increase of PPAR-α protein, target genes of PPAR-α were activated in the liver of core gene transgenic mice; these genes include

cyclin D1, cyclin-dependent kinase (CDK)-4, acy-CoA oxidase, and peroxisome thiolase.[30] However, in general, the activation of PPAR-α leads to improvement but not aggravation of steatosis. Then, what is the function of PPAR-α activation that is observed in the core gene transgenic mice?

To clarify the role of PPAR-α activation in pathogenesis of steatosis and HCC, we mated a core gene transgenic mouse with a PPAR-α knockout (KO) mouse and studied the phenotype. PPAR-α KO mice have reduced expression of target genes of PPAR-α, and have mild steatosis in the liver, as expected.[31] It was unanticipated, however, that steatosis was absent in PPAR-α-null or -heterozygous core gene transgenic mice but present in PPAR-α-intact core gene transgenic mice at the age of 9 or 24 months.[30] 8-Hydroxy deoxyguanosine (8-OHdG) and peroxylipids, both of which are markers for oxidative stress, were decreased in PPAR-α KO core gene transgenic mice. Mitochondrial dysfunction in the core gene transgenic mice, which contributes to overproduction of oxidative stress,[19] was also improved in PPAR-α KO core gene transgenic mice.

Finally, PPAR-α KO core gene transgenic mice did not develop HCC at the age of 24 months, whereas about one-third of PPAR-α-intact core gene transgenic mice did. It should be noted that core gene transgenic mice that are heterozygous for the PPAR-α gene also did not develop HCC.[32] When clofibrate, a peroxisome proliferator, was administered for 24 months to PPAR-α-heterozygous mice, either with or without the core gene, HCC developed in a higher rate in the core gene (+) mice with greater PPAR-α activation. It should be noted that steatosis was present only in core gene (+) PPAR-α-heterozygous mice. In summary, steatosis and HCC developed in PPAR-α-intact but not in PPAR-α-heterozygous or PPAR-α-null core gene transgenic mice, indicating that not the presence but the persistent activation of PPAR-α would be important in hepatocarcinogenesis by HCV core protein. In general, PPAR-α acts to ameliorate steatosis, but with the presence of mitochondrial dysfunction, which is also provoked by the core protein, the core-activated PPAR-α may exacerbate steatosis. Persistent activation of PPAR-α with "strong" ligands such as the core protein of HCV could be carcinogenic in humans, although the low-affinity fibrate ligands are not likely associated with human cancers.

HCV core protein causes "fatty acid spiral"

Figure 2 illustrates our current hypothesis for the role of lipid metabolism in HCV-associated hepatocarcinogenesis. Immune-mediated inflammation should also play a pivotal role in hepatocarcinogenesis in HCV infection. However, in HCV infection, the core protein induces steatosis through the aforementioned pathways, leading to "fatty acid spiral" in the presence of the mitochondrial complex 1 dysfunction and PPAR-α activation, both of which are caused by the core protein. These intracellular alterations would contribute to hepatocarcinogenesis by inducing oxidative stress overproduction and cell-growth signal activation. In such a sense, the core protein of HCV is not a classical-type oncoprotein, but rather seems to contribute to hepatocarcinogenesis by modulating intracellular metabolism and signaling.

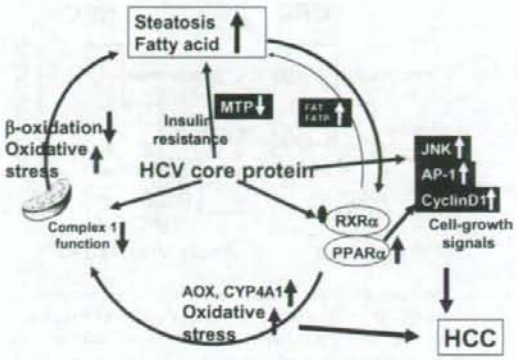

Fig. 2. "Fatty acid spiral" by HCV core protein. In HCV infection, the core protein induces steatosis via several pathways, leading to "fatty acid spiral" in the presence of the mitochondrial complex 1 dysfunction and PPAR-α activation, both of which are also caused by the core protein. These intracellular alterations would contribute to hepatocarcinogenesis by inducing oxidative stress overproduction and cell-growth signal activation. In such a sense, the core protein of HCV is not a classical type oncoprotein, but rather seems to contribute to hepatocarcinogenesis by modulating intracellular metabolism and signaling. *HCV*, hepatitis C virus; *HCC*, hepatocellular carcinoma; *ROS*, reactive oxygen species; *JNK*, c-Jun N-terminal kinase; *ERK*, extracellular signal-regulated kinase; *AP-1*, activating protein-1; *RXR-α*, retinoid X receptor-α; *PPAR-α*, peroxisome proliferator activated receptor-α; *AOX*, acyl-CoA oxidase; *CYP*, cytochrome P450; *MTP*, microsomal triglyceride transfer protein; *FAT*, fatty acid translocase; fatty acid transport protein

The HCV protein may allow some steps in multistep hepatocarcinogenesis to be skipped

The results of our studies on transgenic mice have indicated a carcinogenic potential of the HCV core protein in vivo; thus, HCV would be directly involved in hepatocarcinogenesis. In research studies of carcinogenesis, the theory outlined by Kinzler and Vogelstein[33] has gained wide popularity. They have proposed that the

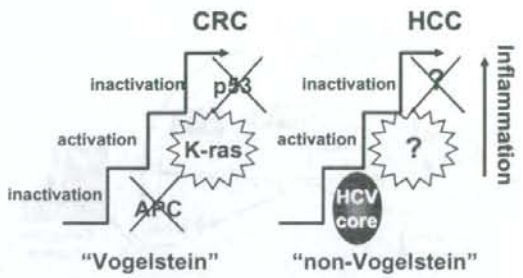

Fig. 3. Mechanism of HCV-associated hepatocarcinogenesis. Multiple steps are required in the induction of all cancers; it would be mandatory for hepatocarcinogenesis that genetic mutations accumulate in hepatocytes. However, in HCV infection, some of these steps may be skipped in the development of HCC in the presence of the core protein. The overall effects achieved by the expression of the core protein would be the induction of HCC, even in the absence of a complete set of genetic aberrations required for carcinogenesis. By considering such a "non-Vogelstein-type" process for the induction of HCC, a plausible explanation may be given for many unusual events happening in HCV carriers

development of colorectal cancer is induced by the accumulation of a complete set of cellular gene mutations. They have deduced that mutations in the APC gene for inactivation, those in K-*ras* for activation, and those in the p53 gene for inactivation accumulate, which cooperate toward the development of colorectal cancer.[33] Their theory has been extended to the carcinogenesis of other cancers as well, called "Vogelstein-type" carcinogenesis (Fig. 3).

On the basis of the results we obtained for the induction of HCC by the HCV core protein, we would like to introduce a different mechanism for hepatocarcinogenesis in HCV infection. We do allow multistages in the induction of all cancers; it would be mandatory for hepatocarcinogenesis that many mutations accumulate in hepatocytes. Some of these steps, however, may be skipped in the development of HCC in HCV infection to which the core protein would contribute (see Fig. 3). The overall effect achieved by the expression of the viral protein would be the induction of HCC, even in the absence of a complete set of genetic aberrations required for carcinogenesis.

By considering such a "non-Vogelstein-type" process for the induction of HCC, a plausible explanation may be given for many unusual events happening in HCV carriers.[34] Now it does not seem so difficult as before to determine why HCC develops in persistent HCV infection at an outstandingly high incidence. Our theory may also give an account of the nonmetastatic and multicentric de novo occurrence characteristics of HCC, which would be the result of persistent HCV infection.

References

1. Saito I, Miyamura T, Ohbayashi A, Harada H, Katayama T, Kikuchi S, et al. Hepatitis C virus infection is associated with the development of hepatocellular carcinoma. Proc Natl Acad Sci USA 1990;87:6547–9.
2. Ikeda K, Saitoh S, Suzuki Y, Kobayashi M, Tsubota A, Koida I, et al. Disease progression and hepatocellular carcinogenesis in patients with chronic viral hepatitis: a prospective observation of 2215 patients. J Hepatol 1998;28:930–8.
3. Okuse C, Yotsuyanagi H, Koike K. Hepatitis C as a systemic disease: virus and host immunologic responses underlie hepatic and extrahepatic manifestations. J Gastroenterol 2007;42:857–65.
4. Koike K, Moriya K. Metabolic aspects of hepatitis C: steatohepatitis distinct from NASH. J Gastroenterol 2005;40:329–36.
5. Negro F. Insulin resistance and HCV: will new knowledge modify clinical management? J Hepatol 2006;45:514–9.
6. Powell EE, Jonsson JR, Clouston AD. Steatosis: co-factor in other liver diseases. Hepatology 2005;42:5–13.
7. Kiyosawa K, Sodeyama T, Tanaka E, Gibo Y, Yoshizawa K, Nakano Y, et al. Interrelationship of blood transfusion, non-A, non-B hepatitis and hepatocellular carcinoma: analysis by detection of antibody to hepatitis C virus. Hepatology 1990;12:671–5.
8. Yotsuyanagi H, Shintani Y, Moriya K, Fujie H, Tsutsumi T, Kato T, et al. Virological analysis of non-B, non-C hepatocellular carcinoma in Japan: frequent involvement of hepatitis B virus. J Infect Dis 2000;181:1920–8.
9. Moriya K, Yotsuyanagi H, Shintani Y, Fujie H, Ishibashi K, Matsuura Y, et al. Hepatitis C virus core protein induces hepatic steatosis in transgenic mice. J Gen Virol 1997;78:1527–31.
10. Moriya K, Fujie H, Shintani Y, Yotsuyanagi H, Tsutsumi T, Matsuura Y, et al. Hepatitis C virus core protein induces hepatocellular carcinoma in transgenic mice. Nat Med 1998;4:1065–8.
11. Koike K, Moriya K, Ishibashi K, Matsuura Y, Suzuki T, Saito I, et al. Expression of hepatitis C virus envelope proteins in transgenic mice. J Gen Virol 1995;76:3031–8.
12. Koike K, Moriya K, Yotsuyanagi H, Shintani Y, Fujie H, Ishibashi K, et al. Sialadenitis resembling Sjögren's syndrome in mice transgenic for hepatitis C virus envelope genes. Proc Natl Acad Sci USA 1997;94:233–6.
13. Bach N, Thung SN, Schaffner F. The histological features of chronic hepatitis C and autoimmune chronic hepatitis: a comparative analysis. Hepatology 1992;15:572–7.
14. Lerat H, Honda M, Beard MR, Loesch K, Sun J, Yang Y, et al. Steatosis and liver cancer in transgenic mice expressing the structural and nonstructural proteins of hepatitis C virus. Gastroenterology 2002;122:352–65.
15. Naas T, Ghorbani M, Alvarez-Maya I, Lapner M, Kothary R, De Repentigny Y, et al. Characterization of liver histopathology in a transgenic mouse model expressing genotype 1a hepatitis C virus core and envelope proteins 1 and 2. J Gen Virol 2005;86:2185–96.
16. Machida K, Cheng KT, Lai CK, Jeng KS, Sung VM, Lai MM. Hepatitis C virus triggers mitochondrial permeability transition with production of reactive oxygen species, leading to DNA damage and STAT3 activation. J Virol 2006;80:7199–207.
17. Moriya K, Fujie H, Yotsuyanagi H, Shintani Y, Tsutsumi T, Matsuura Y, et al. Subcellular localization of hepatitis C virus structural proteins expressed in transgenic liver. Jpn J Med Sci Biol 1997;50:169–77.
18. Sasaki Y. Does oxidative stress participate in the development of hepatocellular carcinoma? J Gastroenterol 2006;41:1135–48.
19. Moriya K, Nakagawa K, Santa T, Shintani Y, Fujie H, Miyoshi H, et al. Oxidative stress in the absence of inflammation in a mouse model for hepatitis C virus-associated hepatocellular carcinogenesis. Cancer Res 2001;61:4365–70.

20. Moriya K, Todoroki T, Tsutsumi T, Fujie H, Shintani Y, Miyoshi H, et al. Increase in the concentration of carbon 18 monounsaturated fatty acids in the liver with hepatitis C: analysis in transgenic mice and humans. Biophys Biochem Res Commun 2001;281: 1207–12.
21. Okuda M, Li K, Beard MR, Showalter LA, Scholle F, Lemon SM, Weinman SA. Mitochondrial injury, oxidative stress, and antioxidant gene expression are induced by hepatitis C virus core protein. Gastroenterology 2002;122:366–75.
22. Tsutsumi T, Suzuki T, Moriya K, Yotsuyanagi H, Shintani Y, Fujie H, et al. Intrahepatic cytokine expression and AP-1 activation in mice transgenic for hepatitis C virus core protein. Virology 2002;304:415–24.
23. Tsutsumi T, Suzuki T, Moriya K, Shintani Y, Fujie H, Miyoshi H, et al. Hepatitis C virus core protein activates ERK and p38 MAPK in cooperation with ethanol in transgenic mice. Hepatology 2003;38:820–8.
24. Miyamoto H, Moriishi K, Moriya K, Murata S, Tanaka K, Suzuki T, et al. Hepatitis C virus core protein induces insulin resistance through a PA28γ-dependent pathway. J Virol 2007;81:1727–35.
25. Shintani Y, Fujie H, Miyoshi H, Tsutsumi T, Kimura S, Moriya K, et al. Hepatitis C virus and diabetes: direct involvement of the virus in the development of insulin resistance. Gastroenterology 2004;126:840–8.
26. Perlemuter G, Sabile A, Letteron P, Vona G, Topilco A, Koike K, et al. Hepatitis C virus core protein inhibits microsomal triglyceride transfer protein activity and very low density lipoprotein secretion: a model of viral-related steatosis. FASEB J 2002; 16:185–94.
27. Moriishi K, Mochizuki R, Moriya K, Miyamoto H, Mori Y, Abe T, et al. Critical role of PA28γ in hepatitis C virus-associated steatogenesis and hepatocarcinogenesis. Proc Natl Acad Sci USA 2007;104:1661–6.
28. Tsutsumi T, Suzuki T, Shimoike T, Moriya K, Yotsuyanagi H, Matsuura Y, et al. Interaction of hepatitis C virus core protein with retinoid X receptor-α modulates its transcriptional activity. Hepatology 2002;35:937–46.
29. Peters JM, Cheung C, Gonzalez FJ. Peroxisome proliferator-activated receptor-alpha and liver cancer: where do we stand? J Mol Med 2005;83:774–85.
30. Tanaka N, Moriya K, Kiyosawa K, Koike K, Aoyama T. Hepatitis C virus core protein induces spontaneous and persistent activation of peroxisome proliferator-activated receptor alpha in transgenic mice: implications for HCV-associated hepatocarcinogenesis. Int J Cancer 2008;122:124–31.
31. Akiyama TE, Sakai S, Lambert G, Nicol CJ, Matsusue K, Pimprale S, et al. Conditional disruption of the peroxisome proliferator-activated receptor gamma gene in mice results in lowered expression of ABCA1, ABCG1, and apoE in macrophages and reduced cholesterol efflux. Mol Cell Biol 2002;22: 2607–19.
32. Tanaka N, Moriya K, Kiyosawa K, Koike K, Gonzalez FJ, Aoyama T. PPAR-α is essential for severe hepatic steatosis and hepatocellular carcinoma induced by HCV core protein. J Clin Invest 2008;118:683–94.
33. Kinzler KW, Vogelstein B. Lessons from hereditary colorectal cancer. Cell 1996;87:159–70.
34. Koike K. Molecular basis of hepatitis C virus-associated hepatocarcinogenesis: lessons from animal model studies. Clin Gastroenterol Hepatol 2005;3:S132–5.

THE JOURNAL OF BIOLOGICAL CHEMISTRY VOL. 284, NO. 6, pp. 3513–3520, February 6, 2009

A Single Amino Acid of Toll-like Receptor 4 That Is Pivotal for Its Signal Transduction and Subcellular Localization*

Received for publication, April 22, 2008, and in revised form, October 29, 2008 Published, JBC Papers in Press, December 8, 2008, DOI 10.1074/jbc.M803086200

Shintaro Yanagimoto[‡§¶], Keita Tatsuno[§], Shu Okugawa[§], Takatoshi Kitazawa[§], Kunihisa Tsukada[§], Kazuhiko Koike[§], Tatsuhiko Kodama[¶], Satoshi Kimura[‖], Yoshikazu Shibasaki[‡†], and Yasuo Ota[1,2]**

From the [‡]Center for Structuring Life Sciences, Graduate school of Arts and Sciences, University of Tokyo, Meguro-ku, Tokyo 153-8903, the [§]Department of Infectious Diseases, Graduate School of Medicine, University of Tokyo, Bunkyo-ku, Tokyo 113-8655, the [¶]Laboratory for Systems Biology and Medicine, Research Center for Advanced Science and Technology, University of Tokyo, Meguro-ku, Tokyo 153-8904, the [‖]Tokyo Teishin Hospital, Fujimi, Chiyoda-ku, Tokyo 102-8798, and the [**]Department of Medicine, Teikyo University School of Medicine, 2-11-1, Kaga, Itabashi-ku, Tokyo 173-8605, Japan

Toll-like receptor 4 (TLR4) is essential for recognizing a Gram-negative bacterial component, lipopolysaccharide (LPS). A single amino acid mutation at position 712 of murine TLR4 leads to hyporesponsiveness to LPS. In this study we determined that an amino acid, a leucine at position 815 of human TLR4, is also pivotal for LPS responsiveness and subcellular distribution. By replacing the leucine with alanine, the mutant TLR4 lost responsiveness to LPS and did not localize on the plasma membrane. In addition, it does not coprecipitate with myeloid differentiation-2, an accessory protein that is necessary for TLR4 to recognize LPS. These results suggest that the leucine at position 815 is required for the normal maturation of TLR4 and for formation of the TLR4·MD-2 complex.

Toll-like receptors (TLRs)[3] play essential roles in both innate and adaptive immunity (1). Thirteen members of the TLR family have been identified in mammals. TLRs have leucine-rich-repeats in their extracellular domains and a Toll/Interleukin-1 receptor (TIR) in their cytoplasmic domains, the latter of which mainly mediates intracellular signaling. Signaling pathways of TLRs, except for TLR3, depend on an adapter protein, MyD88 (myeloid differentiation factor 88), which interacts with the TIR domain of TLRs. This pathway leads to the activation of the transcription factor NF-κB and production of cytokines such as tumor necrosis factor-α and interleukin-6. Another important signaling pathway mediated by TLR3 and TLR4 that exploits the TIR domain is the MyD88-independent pathway. This pathway involves different adapter proteins, such as the TIR domain-containing adaptor inducing interferon-β (TRIF) and TRIF-related adaptor molecule (2–4), and is essential for production of type I interferon through activation of interferon regulatory factor-3.

TLRs recognize as ligands several microbial pathogen-associated molecular patterns. One such pathogen-associated molecular pattern is lipopolysaccharide (LPS), which is recognized by TLR4. LPS triggers severe immunologic reactions by the host in Gram-negative bacterial infections and has drawn attention in many clinical situations. TLR4 is the first mammalian TLR to be discovered in the context of immunology. TLR4 was identified in the search for the genes responsible for LPS hyporesponsiveness (5, 6). The defect was found to stem from a single amino acid mutation, replacement of proline with histidine at position 712, in the cytoplasmic tail of murine TLR4. The study led to the discovery of the importance of TLR4 in innate immunity.

A variety of cells are activated by LPS stimulation through TLR4. TLR4 forms a receptor complex with an accessory protein, myeloid differentiation-2 (MD-2). MD-2 first associates with TLR4 in the endoplasmic reticulum (ER) and *cis*-Golgi, and both proteins move together to the plasma membrane (7, 8). Upon recognition of LPS, the TLR4·MD-2 complex receives LPS on the cell surface and initiates intracellular signaling. The expression of TLR4 in the absence of MD-2 does not confer full responsiveness to LPS stimuli in experimental cell lines (9). An analysis of MD-2 knockout mice revealed that MD-2 is important not only for LPS sensing but also for cellular distribution of TLR4.

In this study we hypothesized that the cytoplasmic tail of TLR4 contains regions that control both localization and signaling. Using truncation and mutation analysis, and paying particular attention to the TIR domain, we identified a single amino acid that is pivotal for both TLR4 signaling and subcellular distribution. The site we found was on the C-terminal portion of the TIR domain for which no specific function has been yet determined.

* This work was partly supported by the Program of Fundamental Studies in Health Sciences of the National Institute of Biomedical Innovation, by the Focus 21 project of the New Energy and Industrial Technology Development Organization, and by the Special Coordination Fund for Science and Technology from the Ministry of Education, Culture, Sports, Science and Technology. This study was also partly supported by a grant-in-aid from the Ministry of Education, Culture, Sports, Science and Technology (to Y. O.). The costs of publication of this article were defrayed in part by the payment of page charges. This article must therefore be hereby marked "*advertisement*" in accordance with 18 U.S.C. Section 1734 solely to indicate this fact.

[1] Both authors contributed equally to this work.

[2] To whom correspondence should be addressed. Tel.: 81-3-3964-1211 (ext. 1756); Fax: 81-3-3579-6310; E-mail: yasuota-tky@umin.ac.jp.

[3] The abbreviations used are: TLR, Toll-like receptor; TIR, Toll/Interleukin-1 receptor; TRIF, TIR domain-containing adaptor inducing interferon-β; LPS, lipopolysaccharide; MD-2, myeloid differentiation-2; ER, endoplasmic reticulum; GFP, green fluorescent protein; EGFP, enhanced GFP; RLA, relative luciferase activity; Sulfo-NHS-SS-Biotin, sulfosuccinimidyl-2-(biotinamido)ethyl-1,3-dithiopropionate.

EXPERIMENTAL PROCEDURES

Reagents and Other Materials—Lipopolysaccharide (LPS) from *Escherichia coli* O55:B5 was purchased from Sigma-Aldrich and applied without repurification. FLAG- and hexa-histidine (His_6)-tagged human TLR4 expression plasmid (pEFBOS/humanTLR4flaghis) and FLAG- and His_6-tagged human MD-2 expression plasmid (pEFBOS/humanMD-2flaghis) were generous gifts from Dr. Kensuke Miyake (Institute of Medical Science, University of Tokyo, Japan). Human CD14 cDNA plasmid (pCMV6-XL5/humanCD14) was purchased from OriGene (Rockville, MD). Fluorescent protein expression vector pEGFP-N3 was purchased from Clontech (Mountain View, CA). Anti-TLR4 monoclonal antibody (clone HTA125) was purchased from Abcam (Cambridge, MA). Anti-FLAG monoclonal antibody (clone M2) was purchased from Sigma-Aldrich. Anti-*A.v.* (GFP) monoclonal and polyclonal antibodies were purchased from Clontech. Control immunoglobulins for immunoprecipitation were purchased from BD Biosciences (San Jose, CA). Horseradish peroxidase-labeled anti-immunoglobulins antibodies were purchased from Dako (Glostrup, Denmark). BlockAce (DS Pharma Biomedical, Osaka, Japan) solution was used as blocking buffer for Western blotting.

Cell Culture—Human embryonic kidney (HEK) 293T cells were maintained in Dulbecco's modified Eagle's medium (Sigma-Aldrich) containing 10% heat-inactivated fetal bovine serum supplemented with penicillin-streptomycin solution (Invitrogen). FuGENE 6 transfection reagent (Roche Applied Science) was used for transient cotransfection according to the manufacturer's instructions. Culture dishes or plates were prepared to 70% confluence prior to transfection. Cells were used for experiments 36 h later. The transfection conditions were optimized for microscopic observation of the expressed fluorescent protein and were kept unchanged in other experiments.

Expression Vector Subcloning and Mutagenesis—Wild-type TLR4 cDNA was excised from pEFBOS/humanTLR4flaghis and subcloned into pEGFP-N3 so that when expressed enhanced green fluorescent protein (EGFP) would be fused at the C terminus of TLR4 (pEGFP-N3/humanTLR4). All mutations were introduced into pEFBOS/humanTLR4flaghis and pEGFP-N3/humanTLR4 using the QuikChange site-Directed mutagenesis kit (Stratagene, La Jolla, CA) according to the manufacturer's instructions and were confirmed by sequencing. For the truncation analysis, two identical unique restriction sites were prepared in the TLR4-coding region of pEFBOS/humanTLR4 using a QuikChange kit, and the DNA fragment to be removed, which was a part of the C terminus of TLR4, was excised enzymatically. After agarose gel purification, the linear double-stranded DNA was ligated to re-form a circular plasmid. Restriction sites were designed so as not to cause a frameshift between TLR4 and EGFP.

Confocal Laser Scanning Microscopy of Cells—Samples were fixed in 3% paraformaldehyde-phosphate-buffered saline at 37 °C for 10 min. Fluorescence images of fixed samples were recorded using a FluoView FV1000 Confocal Microscope (an inverted confocal laser scanning microscope, Olympus, Tokyo, Japan).

Immunoprecipitation—Transfected cells were lysed in lysis buffer (50 mM Tris-HCl, pH 7.5, 100 mM NaCl, 0.1% Triton X-100, 1 mM 1,4-dithiothreitol, and proteinase inhibitor mixture), sonicated, and centrifuged at 4 °C. Antibody was added to the supernatant, and the sample was rotated 1 h at 4 °C followed by the addition of protein G-Sepharose (GE Healthcare Life Sciences, Piscataway, NJ) and an additional 8-h incubation at 4 °C. Bound protein was washed three times in lysis buffer. Proteins were eluted by boiling in SDS sample buffer.

Biotinylation and Purification of Cell Surface Proteins—Prior to surface biotinylation, HEK 293T cells plated in a 100-mm dish were transiently transfected as described above. Surface biotinylation and subsequent purification of biotinylated proteins were performed using a Cell Surface Protein Biotinylation and Purification Kit (Pierce) following the manufacturer's instructions. Briefly, membrane-impermeable sulfosuccinimidyl-2-(biotinamido)ethyl-1,3-dithiopropionate (Sulfo-NHS-SS-Biotin) was added to cell monolayers in the culture dishes and covalently bound to amines in proteins exposed on the cell surface. The affinity resin that binds to the biotin end of Sulfo-NHS-SS-Biotin was used to collect the biotinylated proteins. Reduction by 1,4-dithiothreitol causes cleavage of the disulfide bond in Sulfo-NHS-SS-Biotin, and the elute contains the biotinylated cell surface proteins. Each final sample obtained was considered to contain proteins from an equal amount of cells, because all culture plates were treated equally and grown to full confluence. All samples were sonicated and subjected to SDS-PAGE and Western blotting. The membrane to which protein was transferred was blocked in blocking buffer for 1 h. Then the membrane was incubated with a primary antibody, followed by incubation with horseradish peroxidase-labeled anti-immunoglobulins antibody. The protein bands were then visualized by using a chemiluminescence reagent, Immobilon Western Chemiluminescent HRP Substrate (Millipore, Billerica, MA), according to the manufacturer's instructions.

Cell Stimulation Assays—HEK293T cells were plated and transiently transfected for assays. Thirty-six hours after the transfection, LPS was added to fresh culture medium in each well of the culture plates at the stated concentration. The duration of LPS stimulation was 7 h.

Dual Luciferase Reporter Assays for NF-κB Activation—HEK293T cells were plated in 12-well culture plates (4×10^4 cells/well), and experimental cDNA plasmids were transiently transfected 36 h later using the FuGENE 6 transfection reagent with 0.5 μg of NF-κB reporter plasmid expressing firefly luciferase (pNF-κB-Luc, Stratagene) and 0.05 μg of constitutively active *Renilla* luciferase reporter plasmid (pRL-TK, Promega, Madison, WI) in addition to 0.5 μg each of TLR4-EGFP plasmid and MD-2 plasmid. Stimulation experiments were performed 36 h later. Firefly luciferase and *Renilla* luciferase activities were measured using the Dual-Luciferase Reporter Assay System (Promega) and the Genelight55 luminometer (Microtech, Chiba, Japan). Relative luciferase activity (RLA) was obtained as the ratio of firefly luciferase activity to *Renilla* luciferase activity. Results are expressed as the ratio of RLA with LPS stimulation to RLA without LPS stimulation ([RLA LPS+]/[RLA LPS−]). This ratio should ideally approach 1 when no response to LPS stimulation is observed.

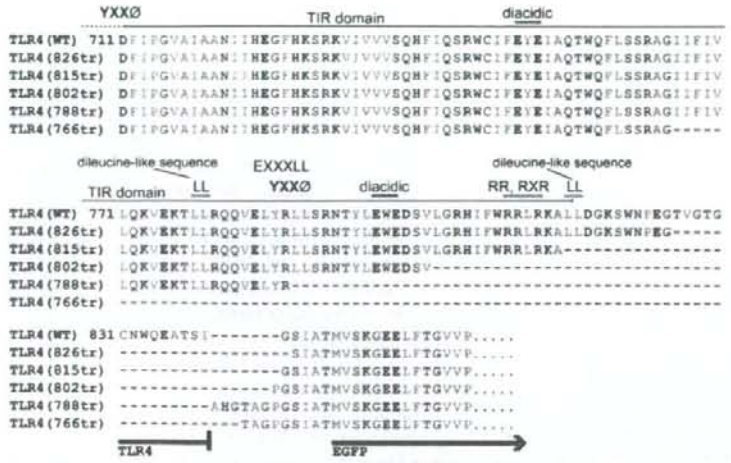

FIGURE 1. **Alignment of the cytoplasmic domains of EGFP fusion TLR4 truncation mutants used in this study.** TLR4 (766tr) signifies the mutant truncated at position 766. Others are named in the same manner. The amino acids are colored based on their physicochemical properties: *pink*, basic; *blue*, acidic; *green*, polar and neutral; and *orange*, hydrophobic. The *black overline* represents the TIR domain. *Colored overlines* indicate amino acid sequences identical to known sorting signal motifs except for two LLs, which are dileucine motif-like sequences in that they consist of solely two consecutive leucines without preceding aspartate or glutamate. *Capital letters* on the *line* signify the single-letter code for amino acids: *E*, glutamic acid; *L*, leucine; *R*, arginine; and *Y*, tyrosine. *X* signifies any amino acid, and Ø signifies an amino acid residue with a bulky hydrophobic side chain.

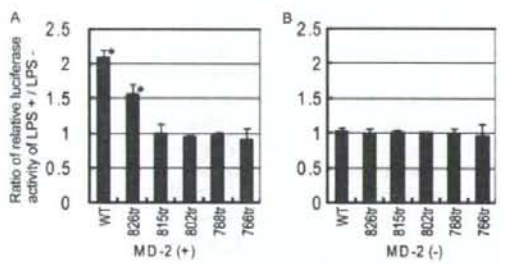

FIGURE 2. **LPS responsiveness measured by NF-κB luciferase assay.** HEK293T cells were transfected with plasmids containing the gene for wild-type TLR4 or a truncated human TLR4-EGFP fusion protein, in addition to a luciferase reporter and human MD-2 plasmid (*A*) or unmodified plasmids (control) (*B*). After 36 h, cells were stimulated with LPS (10 ng/ml) for 7 h, and luciferase reporter gene activity was measured. All results were expressed as the ratio of relative luciferase activity with LPS stimulation to that without stimulation. The data were from three independent experiments. *Small bars* indicate 95% confidence intervals of the mean (*p* values for * are: TLR4 (WT)-EGFP/MD-2 (+), $p = 0.002$; TLR4 (826tr)-EGFP/MD-2 (+), $p = 0.016$).

Statistical Analyses—All quantitative experiments were repeated three times, and each experiment was done in triplicate. The ratio of relative luciferase activity of LPS+ to LPS− was calculated as the index of the responsiveness to the stimuli as explained above. When positive response is observed, the ratio should significantly exceed one. The means of the ratio were represented in *bar graphs*. The 95% confidence interval of the mean of the ratio was calculated and indicated on each *bar* in the *graph*, and *p* values were calculated using Student's *t* distribution compared with the hypothetical mean, one.

RESULTS

Truncation Analysis of TLR 4—To identify amino acid sequences in the cytoplasmic tail of TLR4 that are involved in both signal transduction and subcellular distribution, first we generated five truncation mutants of TLR4 with a fluorescent protein (EGFP) at the C terminus of TLR4.

Although there are no known definite sorting signal motifs in the cytoplasmic tail of TLR4, some amino acid sequences are similar or identical to known general sorting signal motifs as shown in Fig. 1. *YXXØ*, a form of tyrosine-based sorting signal, and *EXXXLL*, a form of dileucine (LL)-based sorting signal, both control protein internalization, lysosomal targeting, and basolateral targeting (10), where "*X*" represents any amino acid, "*Ø*" stands for an amino acid residue with a bulky hydrophobic side chain, and other letters are single-letter abbreviations for the amino acids. "Diacidic" signals such as *DXE* mediate export from the ER (11). RR or *RXR* is another example of an ER export signal (12). Truncation sites were chosen so that some of these amino acid sequences were deleted in each mutant. Because the TIR domain, which is essential in TLR4 signaling and possibly subcellular localization (13), spans most of the cytoplasmic domain of TLR4, four out of five mutants have involvement in the TIR domain, which we hypothesized could result in impaired signal transduction and a change in subcellular distribution. Part of the cytoplasmic portion of the amino acid sequence of the truncation mutants is shown in Fig. 1. The five truncation mutant proteins lost their C-terminal tails at positions 826, 815, 802, 788, and 766, respectively, and were conjugated with EGFP *in vitro*. Actual truncation and ligation sites of all actual mutants were confirmed to have the designed DNA alignment by sequencing.

We utilized the luciferase reporter assay to assess NF-κB transcription activity as an indicator of TLR4 response to LPS stimuli. MD-2 is reported to be essential for this response (9). However, because it is not known whether MD-2 is necessary for transduction of the truncated TLR4 signal as well, we performed the assays with and without MD-2. The index of cell responsiveness to the stimulation was measured as the ratio between RLA with LPS stimulation and RLA without LPS stimulation. Only cells transfected with TLR4 (826tr)-EGFP in combination with MD-2 retained responsiveness to LPS stimulation. One exception was wild-type TLR4-EGFP (Fig. 2*A*). HEK293T cells transfected with TLR4 but without MD-2 did not respond to LPS stimuli regardless of the TLR4-EGFP genotype (Fig. 2*B*).

Next, we compared the localization of wild-type and truncated mutants of TLR4-EGFP in HEK293T by fluorescence microscopy (Fig. 3*A*). The wild-type TLR4 cotransfected with MD-2 was expressed on the plasma membrane and also in the

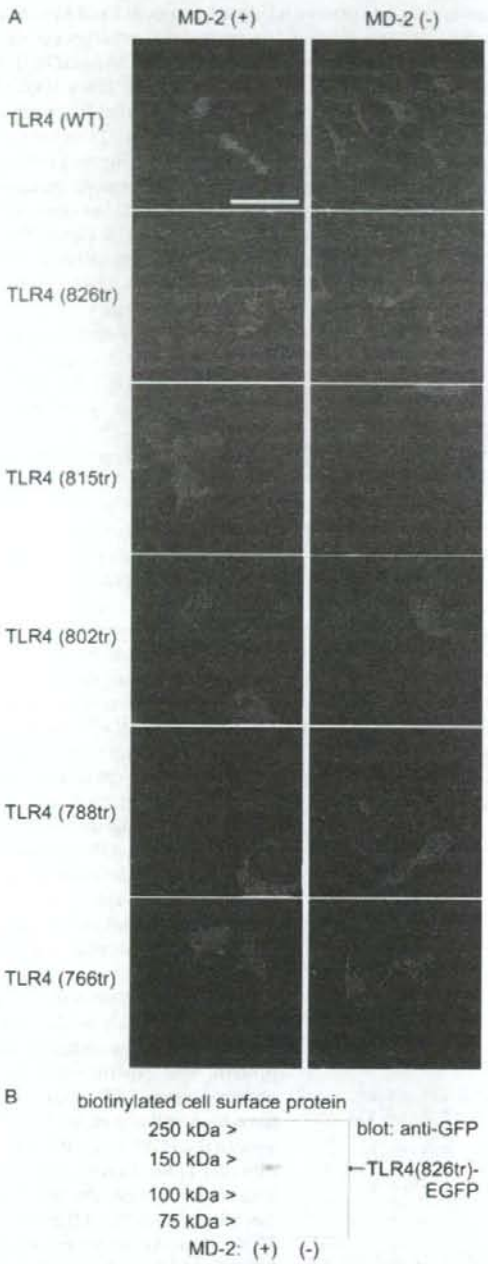

FIGURE 3. **Residues 815–826 of TLR4 contain a region necessary for plasma membrane localization.** *A*, cells were cultured on coverslips in 12-well plates and transfected as in Fig. 2. EGFP-tagged TLR4 was visualized by laser confocal microscopy. Fluorescence from EGFP was observed in *green*. Each genotype of TLR4-EGFP was cotransfected with a human MD-2 plasmid or empty vector. *Bar*, 20 μm. *B*, TLR4 (826tr)-EGFP with or without coexpression of MD-2 were tagged by biotinylation of the cell surface proteins and affinity-purified. TLR4 was visualized by immunoblotting using an anti-GFP monoclonal antibody. Samples from both combinations of DNAs were prepared from the same number of cells.

perinuclear area. These findings were consistent with observations by others (14, 15). TLR4 is reported to localize in the Golgi apparatus as well as on the plasma membrane. Our observation of TLR4-EGFP accumulation in the perinuclear area does not contradict the report that TLR4 partly localizes in the Golgi apparatus (14).

TLR4-EGFP truncation mutants, 815tr, 802tr, 788tr, and 766tr apparently did not localize at the plasma membrane. No particular fluorescence pattern that might be characteristic of localization to a specific intracellular compartment was observed. Only TLR4 (826tr)-EGFP, which has the shortest truncation, was expressed on the plasma membrane and in the perinuclear area, and the fluorescence pattern was similar to that of wild-type (Fig. 3*A*). No TLR4 genotypes, including wild-type TLR4-EGFP, clearly localized on the plasma membrane in the absence of MD-2 (Fig. 3*A*). MD-2 is reported to be necessary for localization of wild-type TLR4 at the plasma membrane (15), which is consistent with our observation. Intracellular distribution of mutant TLR4 varied depending on the genotype, but no particular cellular structure was identified as an alternative target site. Furthermore, we examined the plasma membrane expression of TLR4 (826tr)-EGFP by cell surface protein biotinylation. The expression level of TLR4 (826tr)-EGFP was markedly decreased without coexpression of MD-2 (Fig. 3*B*), which is compatible with the microscope observation.

Removal of the C-terminal segment of TLR4 at residue 826 does not qualitatively affect LPS responsiveness and subcellular distribution. However, when more residues, up to position 815, were removed, both signal transduction and plasma membrane localization were impaired. These results suggest that residues 815–826 of TLR4 contain at least one segment that is critical for those functions.

Amino Acid Sequence Replacement Analysis—To identify critical amino acid sequences in this region, we generated an amino acid replacement mutant of TLR4 instead of truncation mutants. As shown in Fig. 1, although it is not a canonical sequence, leucine-leucine at 815–816 partially fits a known sorting signal motif, a dileucine motif, (D/E)*XXX*L(L/I) or D*XX*LL, which plays an important role in internalization of plasma membrane protein or sorting from the *trans*-Golgi network (10). Thus, as has been done in a similar study (16), a mutant was generated in which alanines were substituted for both leucines at positions 815 and 816.

We measured the NF-κB activity of TLR4 (L815AL816A)-EGFP, the mutant in which both leucines were replaced with alanines, under LPS stimulation (Fig. 4*A*). This mutant protein did not respond to LPS stimuli. Microscopic observation revealed that TLR4 (L815AL816A)-EGFP was not expressed on the plasma membrane regardless of whether MD-2 was cotransfected (Fig. 4*B*). The phenotype of this doubly substituted mutant appeared to be the same as that of the truncation mutants. These results imply that the leucines in positions 815 and 816 play an important role in TLR4 plasma membrane localization.

Analysis of Single Amino Acid Substitution Mutants—As previously mentioned, the amino acid sequence leucine-leucine at positions 815 and 816 does not completely match the dileucine motif, *i.e.* it lacks a preceding acidic amino acid. Therefore it

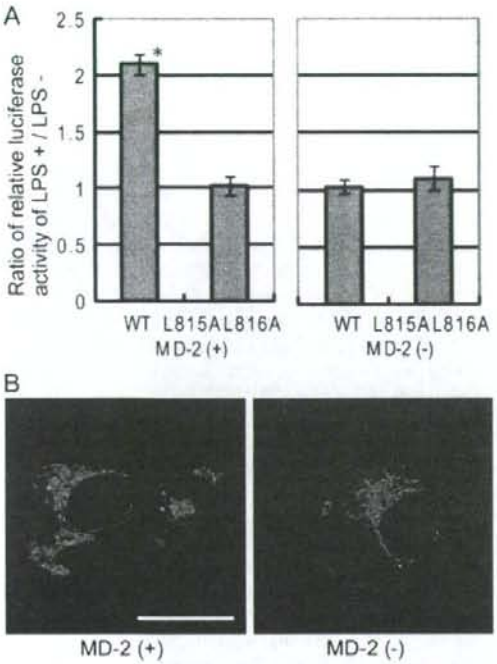

FIGURE 4. **Leucines at positions 815–816 of TLR4 are responsible for impairment of LPS responsiveness and plasma membrane expression.** *A*, the LPS stimulation assay was done for TLR4 (L815AL816A)-EGFP as in Fig. 2. The data were from three independent experiments. *Small bars* indicate 95% confidence intervals of the mean (p value for * are: TLR4 (WT)-EGFP/MD-2 (+), $p = 0.002$). *B*, TLR4 (L815AL816A)-EGFP expression in HEK293T cells was observed by laser confocal microscopy. *Bar*, 20 μm.

was reasonable to explore whether leucines 815 and 816 need to be adjacent to each other. We created five genotypes of single amino acid mutants of TLR4: TLR4 (K813A)-EGFP, TLR4 (L815A)-EGFP, TLR4 (L816A)-EGFP, and TLR4 (D817A)-EGFP. We excluded the amino acid at position 814 from the analysis, because the amino acid in position 814 of wild-type TLR4 is alanine. The amino acid sequence alignment of wild-type TLR4 and the single amino acid replacement mutants is shown in Fig. 5. DNA sequences were confirmed by sequencing.

As was done with truncation mutants, we measured NF-κB activity of wild-type TLR4-EGFP, TLR4 (K813A)-EGFP, TLR4 (L815A)-EGFP, TLR4 (L816A)-EGFP, and TLR4 (D817A)-EGFP in response to LPS stimulation. All mutants except TLR4 (L815A)-EGFP showed responsiveness to LPS stimulation with coexpression of MD-2 (Fig. 6*A*). Without MD-2, no genotype of TLR4-EGFP responded to LPS stimulation (Fig. 6*B*). LPS stimulation was performed in an identical manner as with truncation mutants.

We analyzed the subcellular distribution of single amino acid mutants of TLR4-EGFP with and without MD-2 coexpression by fluorescence microscopy. TLR4 (K813A)-EGFP and TLR4 (D817A)-EGFP showed a similar fluorescence pattern to the wild-type, which localized at the plasma membrane when coexpressed with MD-2. No genotypes of TLR4-EGFP localized on the plasma membrane without MD-2 (Fig. 7). The cells transfected with TLR4 (L815A)-EGFP coexpressed with MD-2 did not show plasma membrane fluorescent pattern. Also, TLR4 (L815A)-EGFP showed comparatively weaker fluoresce than other mutants, possibly due to lower expression of the protein. Fluorescence of TLR4 (L816A)-EGFP with MD-2 was ambiguous as for the plasma membrane expression. Some kind of membranous structure was observed in the cytoplasmic area, but the intensity of the plasma membrane green fluorescence was obscure. Together with the results from the LPS stimulation experiment, the leucines at positions 815 and 816 are considered to play important roles in signal transduction and/or subcellular distribution of TLR4.

FIGURE 5. **Alignment of the cytoplasmic domain of EGFP fusion TLR4 amino acid-replacement mutants used in this study.** TLR4 (L813A) signifies a mutant with leucine replaced with alanine at position 813. Others are named in the same manner. The amino acids are *colored* as in Fig. 1. All amino acids are designated using the single-letter code.

Because EGFP consists of 239 amino acids, which is about one-third the size of the complete TLR4 protein, the experimental results obtained using TLR4-EGFP could have been influenced by the presence of the EGFP fused at the C terminus of TLR4. To rule out this possibility, we tested the functional integrity of both TLR4 (L815A) and TLR4 (L816A) with and without EGFP at the C terminus. Reporter assays were performed under the same conditions except that the shorter tag, FLAG-His_6, which has only 21-amino acid tags at the C terminus, was fused to TLR4 in place of EGFP. There was no difference